iScience

CellPress
OPEN ACCESS

Article

Alleviation of monocyte exhaustion by BCG derivative mycolic acid

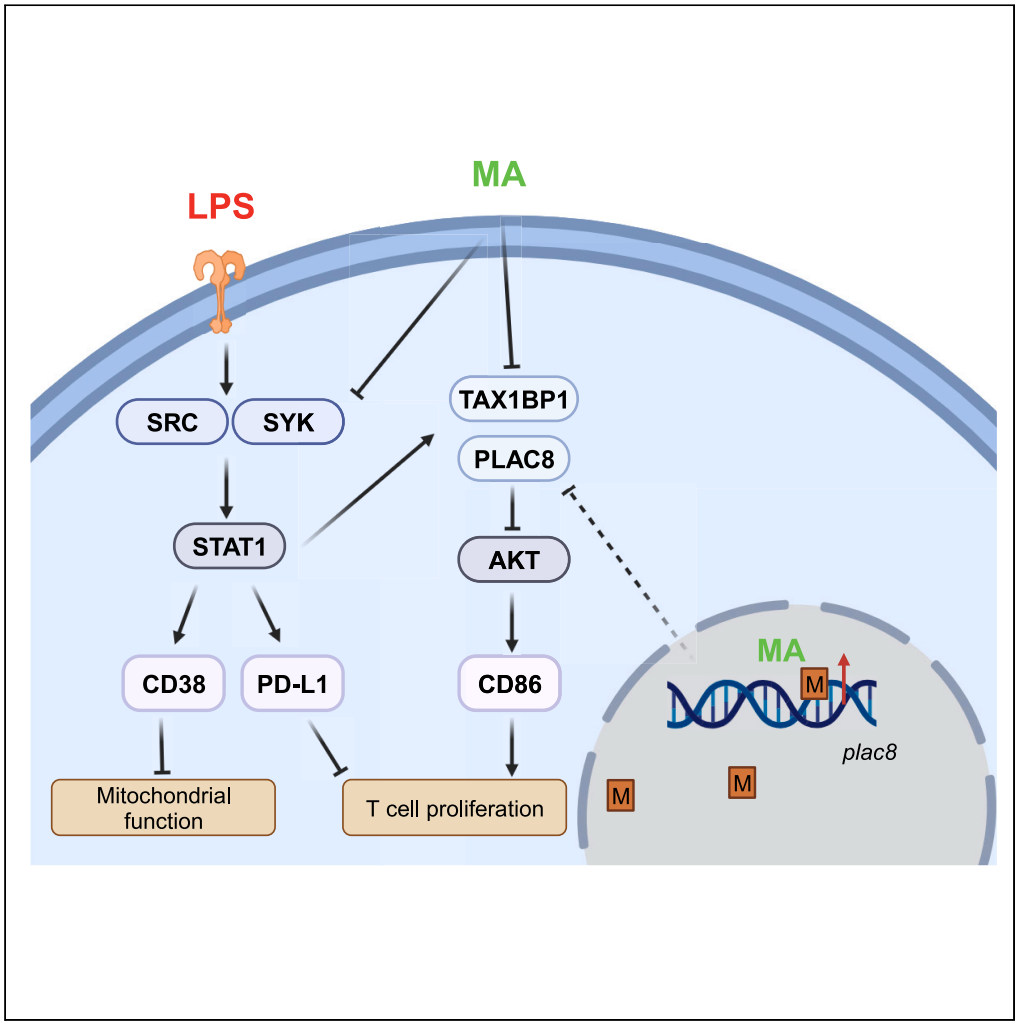

Yajun Wu, Blake Caldwell, Jing Wang, Yao Zhang, Liwu Li

lwli@vt.edu

Highlights

Methoxy-mycolic acid (M-MA) effectively alleviates monocyte exhaustion *in vitro*

M-MA restores immune homeostasis by blocking Ly6C^{hi}/CD38^{hi} monocyte expansion

M-MA treatment rejuvenates mitochondrial function and attenuates T cell suppression

M-MA erases methylation memory in exhausted monocytes

Wu et al., iScience *27*, 108978
February 16, 2024
https://doi.org/10.1016/j.isci.2024.108978

iScience

CellPress
OPEN ACCESS

Article

Alleviation of monocyte exhaustion by BCG derivative mycolic acid

Yajun Wu,[1] Blake Caldwell,[1] Jing Wang,[1] Yao Zhang,[1] and Liwu Li[1,2,*]

SUMMARY

Monocyte exhaustion with sustained pathogenic inflammation and immune-suppression, a hallmark of sepsis resulting from systemic infections, presents a challenge with limited therapeutic solutions. This study identified Methoxy-Mycolic Acid (M-MA), a branched mycolic acid derived from *Mycobacterium bovis* Bacillus Calmette–Guérin (BCG), as a potent agent in alleviating monocyte exhaustion and restoring immune homeostasis. Co-treatment of monocytes with M-MA effectively blocked the expansion of Ly6C^{hi}/CD38^{hi}/PD-L1^{hi} monocytes induced by LPS challenges and restored the expression of immune-enhancing CD86. M-MA treatment restored mitochondrial functions of exhausted monocytes and alleviated their suppressive activities on co-cultured T cells. Independent of TREM2, M-MA blocks Src-STAT1-mediated inflammatory polarization and reduces the production of immune suppressors TAX1BP1 and PLAC8. Whole genome methylation analyses revealed M-MA's ability to erase the methylation memory of exhausted monocytes, particularly restoring Plac8 methylation. Together, our data suggest M-MA as an effective agent in restoring monocyte homeostasis with a therapeutic potential for treating sepsis.

INTRODUCTION

Sepsis, initiated by severe and systemic infections or injuries, is a leading cause of mortality and morbidity for patients in critical units around the world.[1] Emerging basic and clinical studies reveal that exhausted host immune responses characterized by a paradigm of sustained pathogenic inflammation and immune suppression are collectively responsible for the high mortality/morbidity associated with sepsis.[2–4] Sustained pathogenic inflammation leads to damage of multi-organs and tissues, while immune suppression compromises the host defense toward secondary infections.[5,6] Currently, there is a lack of effective strategies to properly block immune exhaustion and restore host immune homeostasis, thus impeding our effort toward the effective treatment of sepsis.

Integrated *in vivo* and *in vitro* studies reveal that host monocytes can adopt the salient features of immune exhaustion during sepsis,[7,8] as characterized by sustained expression of pathogenic inflammatory mediators such as CD38 and immune suppressors such as PD-L1, as well as compromised expression of immune-enhancing mediators such as CD86.[9–11] CD38 is an ectoenzyme responsible for the degradation of nicotinamide adenine dinucleotide (NAD) and the generation of inflammatory secondary metabolites.[12,13] In exhausted monocytes, the NAD level is drastically diminished, resulting in mitochondrial dysfunction.[14] Independent studies indicate that CD38/NAD$^+$ dysregulation is involved in the pathogenesis of both acute and chronic diseases such as diabetes, cardiovascular disease, and sepsis caused by polymicrobial infections including COVID-19.[15–18] PD-L1 is a well-characterized suppressor elevated in septic monocytes responsible for compromising host T cell function.[19,20] On the other hand, immune enhancer CD86 involved in maintaining effective adaptive immune function is drastically reduced in septic monocytes.[21] The key features of pathogenic inflammation and immune suppression can be recapitulated *in vitro* by prolonged treatment with bacterial endotoxin lipopolysaccharide (LPS),[9] providing a robust experimental system to screen potential compounds in effectively restoring monocyte homeostasis.

M. bovis Bacillus Calmette–Guérin (BCG) is a live attenuated vaccine against tuberculosis.[22] Emerging studies suggest that BCG can also provide cross-protection against diverse pathogens unrelated to tuberculosis.[23–25] Mechanistic studies suggest that "trained" innate immunity with immune-enhancing efficacies may be responsible for the broad protective effects of BCG as well as other microbial products such as beta-glucan.[25,26] Trained innate immune cells exhibit enhanced responses in facilitating host defense, decreasing the risk of sepsis or other infectious diseases.[4] Trehalose-6,6-dimycolate (TDM), a unique glycolipid that is glycosylated by mycolic acid (MA) identified in the *Mycobacterium tuberculosis* cell wall, has been used as a vaccine adjuvant to promote and augment the intensity and duration of the immune response.[27,28] Despite these intriguing advances, the beneficial effects of BCG and its TDM derivatives in treating sepsis have not been robustly defined in clinics, due to varying efficacies potentially caused by complex structures and variations of BCG and TDM isolates.

In this current study, we aim to define the effects of highly purified TDM derivative, MA, in modulating monocyte exhaustion. We tested the efficacies of α-MA as well as the branch-chain methoxy-MA (M-MA) in modulating monocyte exhaustion induced by prolonged challenges

[1]Department of Biological Sciences, Virginia Tech; Blacksburg, VA 24061-0910, USA
[2]Lead contact
*Correspondence: lwli@vt.edu
https://doi.org/10.1016/j.isci.2024.108978

with LPS. We observed that M-MA is most potent in blocking monocyte exhaustion and restoring monocyte homeostasis, in both murine and human monocytes. Mechanistically, we examined key cellular signaling circuitries involved in monocyte exhaustion modulated by M-MA. We further performed genome-wide methylation analyses of exhausted monocytes and examined the erasure of imprinted methylation memory by M-MA. Our data suggest that M-MA may serve as a potent agent in restoring monocyte homeostasis.

RESULTS

M-MA alleviates monocyte exhaustion

Although TDM was previously shown to exert some protective effects by inducing "trained" innate immunity and alleviating sepsis severity,[29,30] its highly variable molecular composition may result in inconsistent treatment efficacies in clinical settings that compromise its therapeutic potential. We therefore tested whether highly purified MA derivatives of TDM can have similar effects in blocking monocyte exhaustion and restoring monocyte homeostasis *in vitro*. To achieve this objective, we used the previously defined *in vitro* culture model by selectively maintaining the survival of primary monocytes from bone marrow cells with low-dose M-CSF.[9,31] scRNA-seq as well as flow cytometry analyses confirmed that cells harvested from mouse bone marrow cultured with media supplement with M-CSF selectively enable the survival of monocytes/macrophages but not other hematopoietic cells.[31] Similar long-term *in vitro* culture system with either M-CSF or GM-CSF were independently developed to selectively sustain either monocytes/macrophages, and provide well-controlled systems for examining innate memory development.[32,33] M-CSF maintained bone marrow-derived monocytes (BMDMs) were treated by control PBS, high-dose LPS (100 ng/mL), or high-dose LPS with M-MA (10 μg/mL), α-MA (10 μg/mL) or TDM (10 μg/mL). Fresh complete media with M-CSF and various treatments were supplemented every 2 days as reported previously (Figure 1A).[9,34] Cultured cells were harvested on day 5 for flow cytometry analysis, and our previous analyses confirmed >99% monocytes with this condition.[31] As shown in Figure 1, following 5-day culture, PBS-treated cells were primarily composed of homogeneous populations of homeostatic $CD11b^{+}Ly6C^{-}$ monocytes, whereas cells subjected to prolonged high-dose LPS stimulation shifted toward the $Ly6C^{++}$ and $Ly6C^{+}$ subtypes (Figures 1B–1E) characteristic of exhausted monocytes with pathogenic inflammatory and immune-suppressive functions in animal models of sepsis.[35] By contrast, co-treatment with either TDM or MA during LPS exposure alleviates the expansion of $Ly6C^{++}$ and $Ly6C^{+}$ populations (Figures 1C and 1D) and partially restore the $Ly6C^{-}$ population (Figure 1E) relative to monocytes treated with LPS alone.

We then examined the impact of MA treatment on the expression of key exhaustion markers. In agreement with our previous study, exhausted monocytes express elevated levels of PD-L1 and CD38 and reduced levels of CD86.[9] We observed that only M-MA and TDM treatment reduced the induction of PD-L1 by LPS (Figure 1F) and both MA and TDM partially restored cell surface levels of CD86 in LPS-exhausted monocytes (Figure 1G). Furthermore, we observed that co-treatment with MA or TDM can potently reduce CD38 expression in LPS-exhausted monocytes (Figure 1H). Collectively, these results suggest that, similar to TDM, MA treatment has the potential to resolve many of the pathogenic features of exhausted monocytes during septic challenge. We found that M-MA is much more potent compared to α-MA in restoring monocyte homeostasis, and therefore focused on using M-MA in all subsequent analysis.

We next tested whether M-MA may have similar effects on primary human monocytes. As monocytes from PBMCs are more sensitive to LPS, we exhausted human cells with the lower dose of LPS (50 ng/mL) in the presence or absence of 10 μg/mL M-MA for a one-day culture period. We validated that LPS treatment alone can reduce the population of non-classical $CD14^{lo}$ $CD16^{hi}$ monocytes and expand the classical $CD14^{hi}$ $CD16^{lo}$ monocyte population (Figures S1A–S1C). Co-treatment with M-MA led to a partial restoration of the non-classical monocyte population as compared to LPS treatment alone (Figure S1A). In terms of key exhaustion markers, LPS treatment led to increased expression of PD-L1, and a reduction of CD86 expression on cultured PBMCs, consistent with murine monocytes (Figures S1D and S1E). LPS also significantly increased the levels of CD38 in both the non-classical and intermediate monocytes (Figures S1G and S1H). Co-treatment with MA strongly reduced the expression of PD-L1 and CD38 and restored CD86 on LPS-exhausted human monocytes (Figures S1D, S1E, S1G, and S1H). Taken together, our data reveal that M-MA can effectively block exhaustion and restore homeostasis in both murine and human monocytes.

M-MA treated monocytes exhibit improved mitochondrial integrity and promote T cell proliferation

We next examined the consequences of monocyte functional exhaustion by LPS and restoration by M-MA. CD38, an ectoenzyme involved in the metabolism of NAD, has been implicated in the initiation of pathogenic inflammation of diseases such as diabetes, cardiovascular disease, sepsis, and Covid-19.[15–18] In the context of monocyte exhaustion, increased expression of CD38 leads to a reduction in NAD^{+} levels, resulting in mitochondrial dysfunction and subsequent pathogenic inflammatory processes.[14] To investigate whether M-MA can alleviate oxidative stress in exhausted monocytes by restoring NAD^{+} levels, we assessed intracellular NAD^{+} levels in monocytes co-treated with M-MA and LPS. Whereas NAD^{+} levels were drastically reduced in LPS-exhausted monocytes, they were significantly restored by M-MA co-treatment (Figure 2A). Previous research has also shown that reduced cellular NAD^{+} levels can shift metabolism toward anaerobic respiration via lactic acid fermentation.[14] In our study, we observed increased intracellular lactate levels in LPS-exhausted monocytes, while the co-treatment of M-MA and LPS reduced lactate to the control levels (Figure 2B). To further characterize mitochondrial stress in exhausted monocytes, we evaluated mitochondrial membrane potential using MitoTracker Deep Red (MTDR). LPS-stimulated monocytes showed a substantial decreasing in MTDR intensity and expansion of the MTDR-negative population, indicative of impaired mitochondrial function (Figures 2C and 2D). In contrast, M-MA co-treatment attenuated this effect, restoring the MTDR-positive population (Figure 2D).

To explore potential molecular regulators of mitochondrial function, we measured intracellular levels of PGC-1α using flow cytometry. PGC-1α is a transcriptional coactivator that plays a vital role in facilitating efficient cellular energy metabolism, thereby maintaining mitochondrial biogenesis and cellular NAD levels.[36–38] Increased NAD levels can also serve as positive feedback in sustaining the activation of

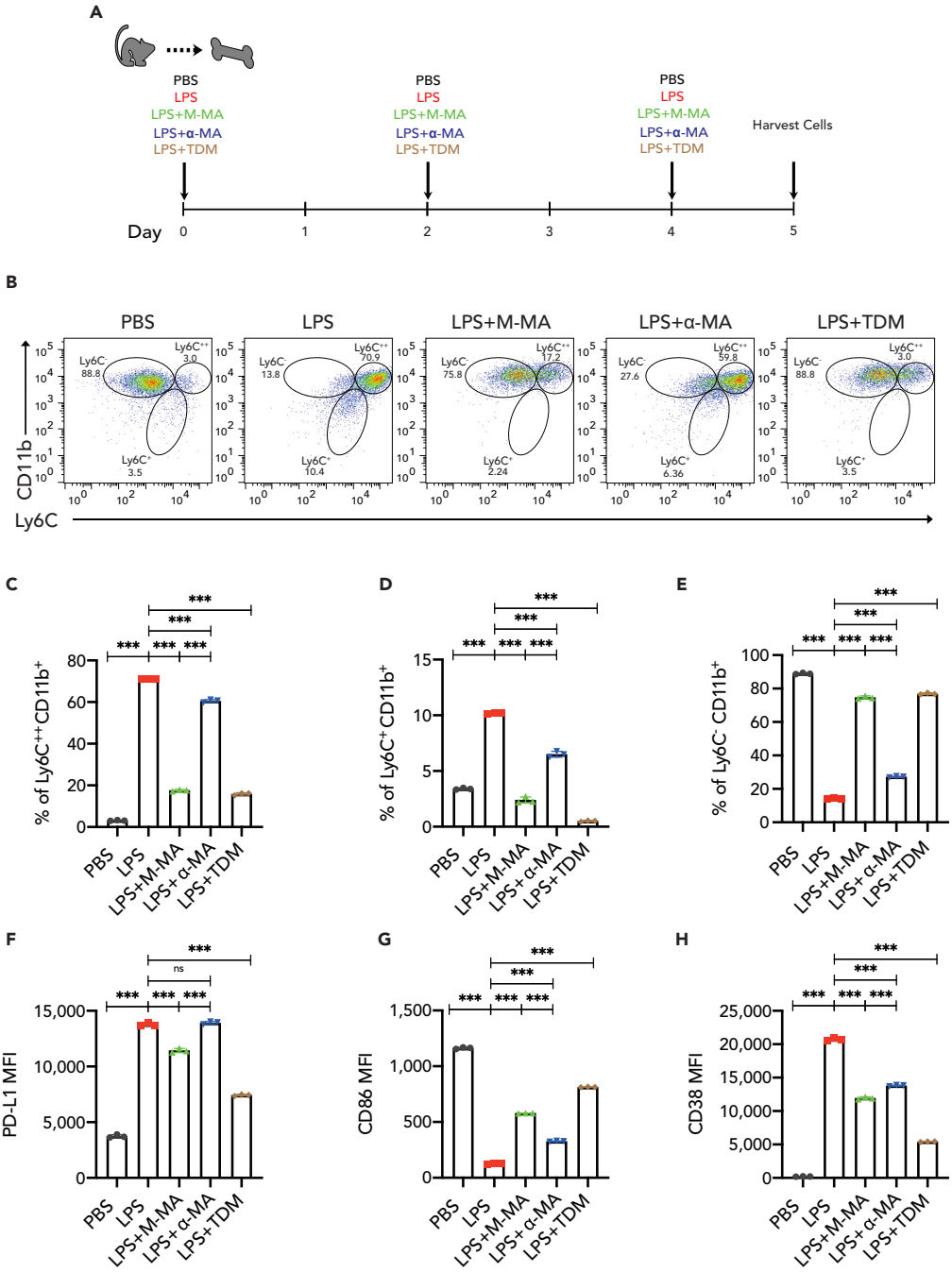

Figure 1. M-MA alleviates monocyte exhaustion

(A) M-CSF maintained BMDMs were treated with PBS, high dose LPS (100 ng/mL), high dose LPS plus M-MA (10 μg/mL), high dose LPS plus α-MA (10 μg/mL), or high dose LPS plus TDM (10 μg/mL) for 5 days.

(B) Flow cytometry analysis was performed to assess the populations of Ly6C^{++} CD11b^{+}, Ly6C^{+} CD11b^{+}, and Ly6C^{-} CD11b^{+} cells in the cell cultures treated with different conditions for 5 days.

(C–E) The percentage of the indicated populations was quantified based on flow cytometry data.

(F–H) The Mean Fluorescent Intensity (MFI) of PD-L1, CD86, and CD38 on day 5 was measured using flow cytometry. The flow data shown are representative of three independent biological replicates, and error bars indicate the means ± standard deviation (SD) with n = 3 for each group. Statistical analysis was performed using one-way ANOVA, ***p < 0.001.

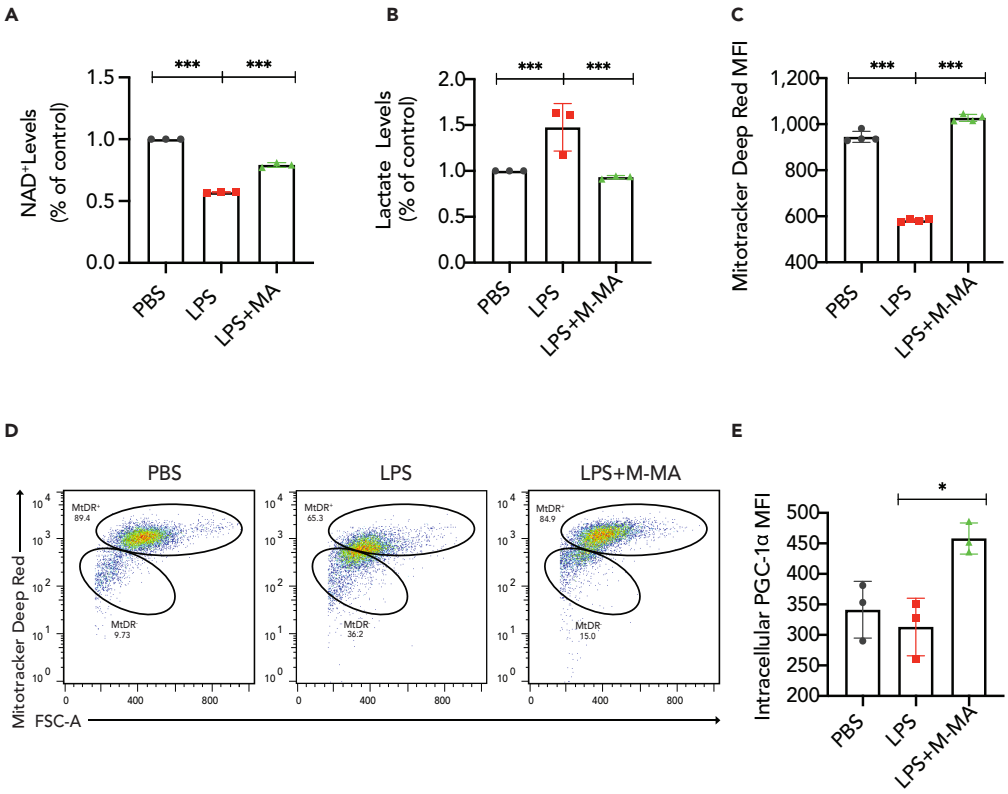

Figure 2. M-MA treatment improves mitochondrial integrity in exhausted monocytes

M-CSF maintained BMDMs were stimulated with PBS, high dose LPS (100 ng/mL) or 100 ng/mL LPS plus 10 μg/mL M-MA for 5 days. NAD+ levels (A) and Lactate levels (B) in monocytes were normalized to the PBS group. To assess the effect of M-MA on mitochondrial potential, monocytes were stained with MitoTracker Deep Red (MTDR).

(C and D) displays the results as both the MFI and the percentage of cells within the population.

(E) The intracellular level of PGC1- α was determined by flow cytometry. The data shown are representative of three independent biological replicates, and error bars indicate the means ± SD with n = 3 for each group. Statistical analysis was performed using one-way ANOVA, *p < 0.05, ***p < 0.001.

PGC-1α.[38] Indeed, we observed a significant increase in PGC-1α levels in M-MA and LPS co-stimulated monocytes relative to LPS-treated monocytes (Figure 2E), consistent with improved mitochondria function.

Due to reduced CD86 and elevated PD-L1 levels, exhausted monocytes can potently suppress T cell functions both *in vitro* and *in vivo*.[39–41] We next tested whether M-MA co-treatment can alleviate the myeloid suppressor functions of exhausted monocytes toward CD4 and CD8 T cells. 5-day pre-treated monocytes were subjected to co-culture assays with CFSE-labeled T cells (Figure 3A). Monocytes exhausted by LPS alone significantly reduced the proliferation of co-cultured CD4 or CD8 T cells (Figures 3B–3D). This inhibitory effect was partially relieved in monocytes treated with both LPS and M-MA (Figures 3B–3D). Additionally, we observed an increased expression of CD69 on both CD8 and CD4 T cells in M-MA and LPS co-treated group, as compared to the group stimulated with LPS alone (Figures 3E and 3F). This provides additional evidence that M-MA co-treated monocytes have the potential to augment T cell activation, thereby increasing T cell proliferation. Thus, our data reveal that M-MA can potently alleviate the myeloid suppressor functions of exhausted monocytes and restore immune homeostasis.

The effects of M-MA in restoring monocyte homeostasis are not dependent upon TREM2

Mechanistically, a previous study reported that TREM2 may serve as a specific cell-surface receptor for mycolic acid.[42] To test whether TREM2 is responsible for mediating the effects of M-MA in restoring monocyte homeostasis, we compared the responses of murine WT and TREM2 KO monocytes in our *in vitro* experimental system as described above. However, addition of M-MA still robustly expanded $Ly6C^{-}$ population and reduced $Ly6C^{++}$ population (Figures 4A–4C) in TREM2 KO monocytes. Likewise, TREM2-deficient monocytes co-treated with LPS and M-MA showed the reduction of CD38 and PD-L1 and restoration of CD86 (Figures 4D–4F), suggesting that the protective effects of M-MA in restoring monocyte homeostasis are not TREM2-dependent.

Additive effects of M-MA with TRAM deletion in restoring monocyte homeostasis

We posit that M-MA may exert its protective effects via generic intervention of cell membrane-mediated stress signaling. TLR4 intracellular adaptors are known to cluster around membrane lipid rafts to assemble signalosomes that mediate signal strength- and history-dependent

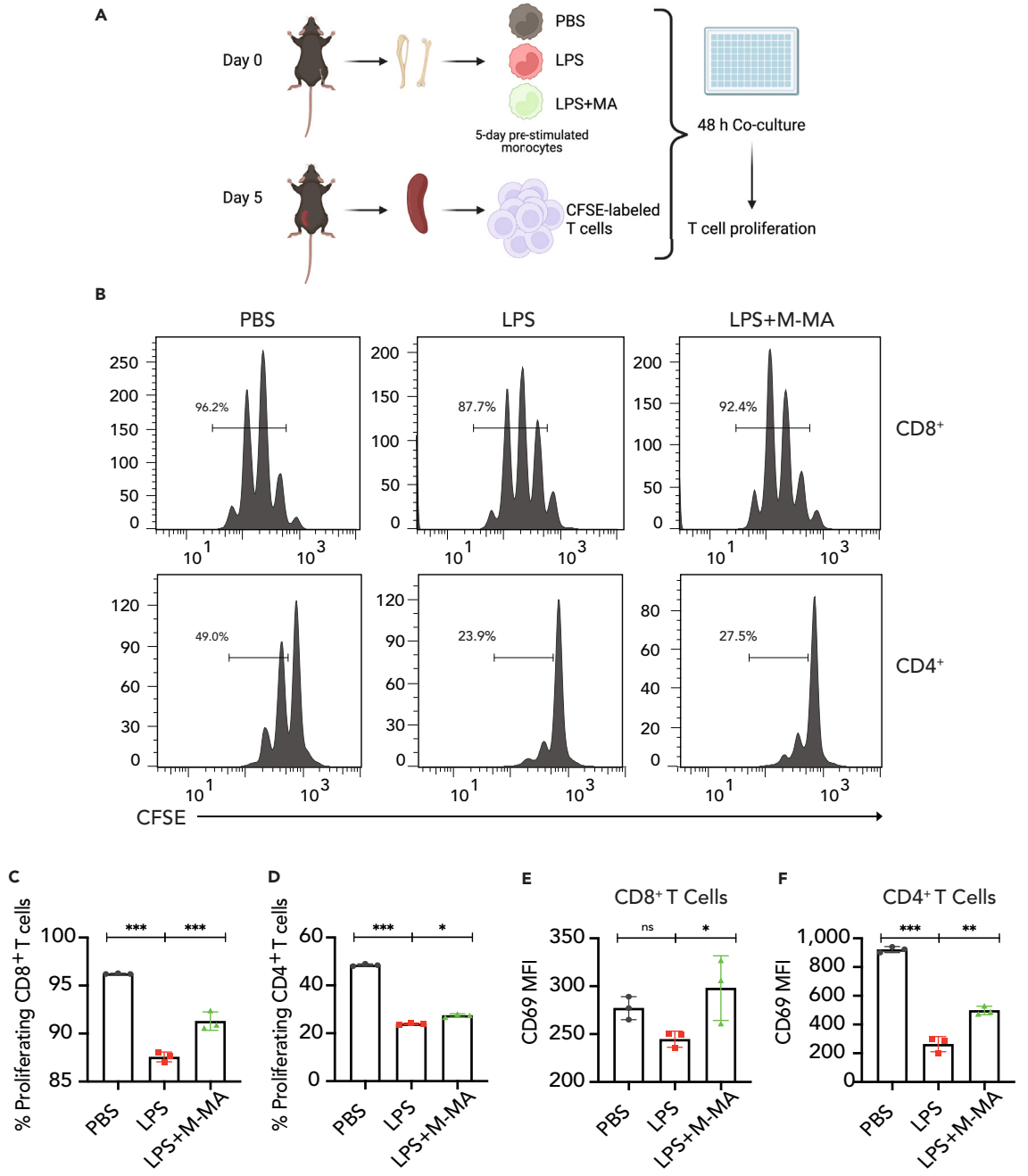

Figure 3. M-MA treatment results in elevated T cell activation and proliferation

(A) T cells isolated from the spleen were pre-labeled with CFSE and cocultured with the treated monocytes for an additional 48 h.

(B) CFSE peaks were indicated in the T cells proliferating generation.

(C and D) The proliferating percentages of CD8 and CD4 T cells were quantified.

(E and F) The MFI of CD69 on CD8 and CD4 T cells was detected by flow cytometry. The data shown are representative of three independent biological replicates, and error bars indicate the means ± SD with n = 3 for each group. Statistical analysis was performed using one-way ANOVA, *p < 0.05, **p < 0.01, ***p < 0.001.

monocyte activation.[43,44] While cholesterol and related lipids can increase membrane rigidity and lipid raft formation, branched fatty acids were shown to reduce membrane rigidity and potentially reduce the incidence of lipid rafts.[45,46] With particular significance, TRAM can be covalently myristoylated and inserted into lipid membrane rafts.[47] Given that TRAM deletion was previously shown to inhibit monocyte exhaustion, we next tested whether the branched methoxy-MA may potentially synergize with TRAM deletion and completely restore monocyte homeostasis.

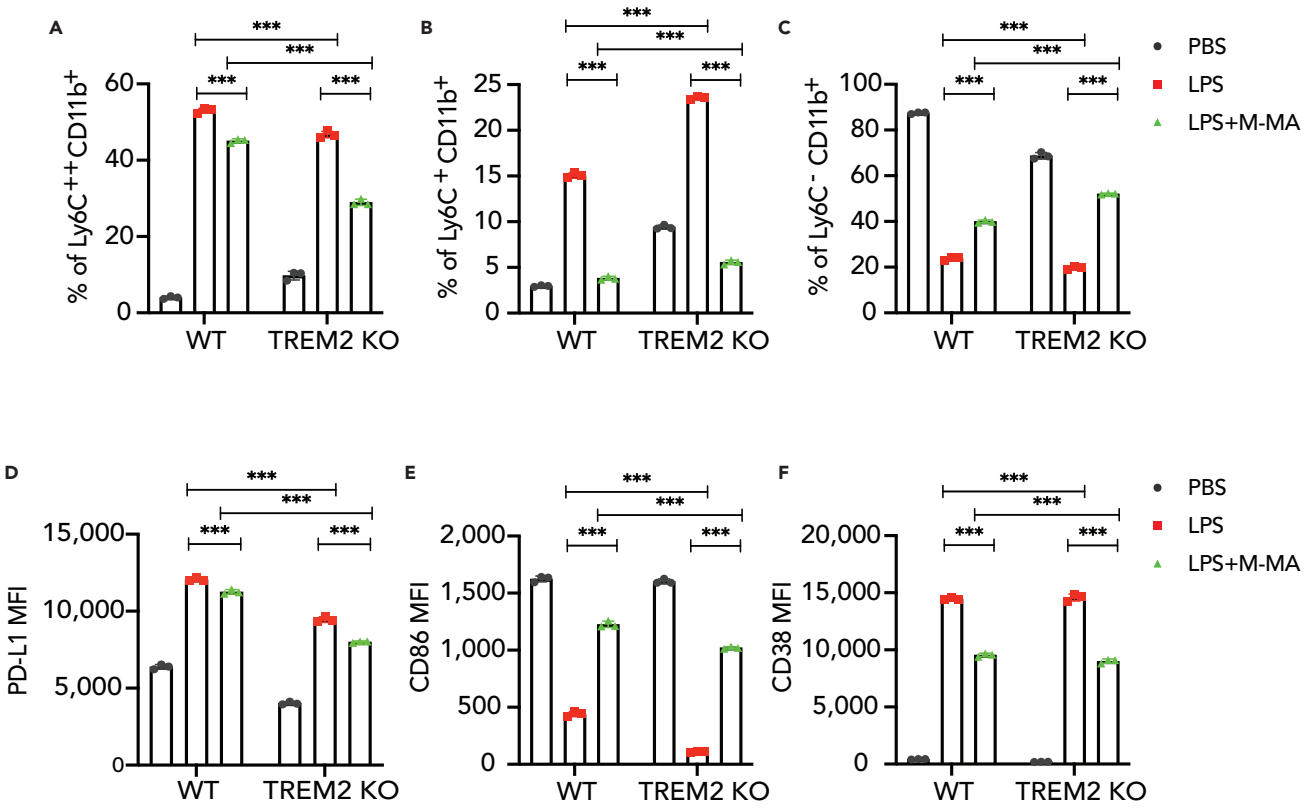

Figure 4. The effects of M-MA in restoring monocyte homeostasis are not dependent upon TREM2

M-CSF maintained BMDMs from WT or TREM2 KO mice were treated with PBS, high dose LPS (100 ng/mL) in the presence of M-MA (10 μg/mL) or without LPS for 5 days.

(A–C) Ly6C^{++} CD11b^{+}, Ly6C^{+} CD11b^{+}, and Ly6C^{-} CD11b^{+} were shown as frequency.

(D–F) The MFI of PD-L1 (D), CD38 (E), and CD86 (F) were measured by flow cytometry. Data represent three independent biological replicates; error bars show means ± SD (n = 3 per group). Statistical analysis: two-way ANOVA, ***p < 0.001.

Consistent with our previous study, we validated that TRAM deletion can drastically reduce monocyte exhaustion induced by persistent LPS challenges. TRAM-deficient monocytes exhibited a dramatically reduced expansion of Ly6C^{++} monocytes, reduced expression of CD38 and PD-L1, and partially restored expression of CD86 compared to WT monocytes (Figures 5A–5F). Although M-MA did not further reduce PD-L1 levels in LPS-treated Tram$^{-/-}$ monocytes (Figure 5D), M-MA co-treatment with LPS further reduced the population of Ly6C^{++} monocytes (Figure 5A) and completely restored the expression of CD86 (Figure 5E). Our data suggest that the effects of M-MA are partially related to blocking TRAM-mediated monocyte exhaustion, and likely involve the relief of additional cellular stress signaling processes.

M-MA potently blocks key signaling circuitry involved in monocyte exhaustion

Next, we tested the effects of M-MA on key intracellular signaling processes involved in monocyte exhaustion. Innate adaptor-mediated activation of Src kinases was shown to induce prolonged activation of STAT1,[48] which can cause sustained induction of pathogenic inflammatory mediators such as CD38 as well as immune-suppressive PD-L1.[49,50] Functionally, elevated STAT1 exacerbates sepsis pathogenesis, and genetic deletion of STAT1 can alleviate sepsis severity.[51,52] Therefore, we tested the effects of M-MA on modulating these key signaling molecules in exhausted monocytes.

As shown in Figures 6A and 6D–6H, monocytes exhausted by prolonged challenges with LPS exhibit robust induction of Src, Syk, and STAT1. In contrast, co-incubation with M-MA significantly reduced the activation of Src, Syk, and STAT1 in monocytes (Figures 6A and 6D–6H).

As a compensatory mechanism, exhausted monocytes challenged with prolonged LPS stimulation exhibit elevated autophagy-mediated suppression of Akt and NF-κB.[53] Reanalyzing our previously published monocyte exhaustion scRNA-seq dataset,[9] we found that exhausted monocytes express high levels of *Tax1bp1* and *Plac8*, both of which are involved in autophagy-mediated suppression of Akt and NF-κB through targeting TBK1.[54,55] Elevated PLAC8 levels were also independently reported in monocytes collected from experimental septic animals and septic patients.[56–58] We confirmed via western blot that TAX1BP1 is robustly induced in exhausted monocytes, and that this induction was blocked by the co-treatment with M-MA (Figures 6B and 6I). Likewise, we validated the induction of PLAC8 in exhausted monocytes

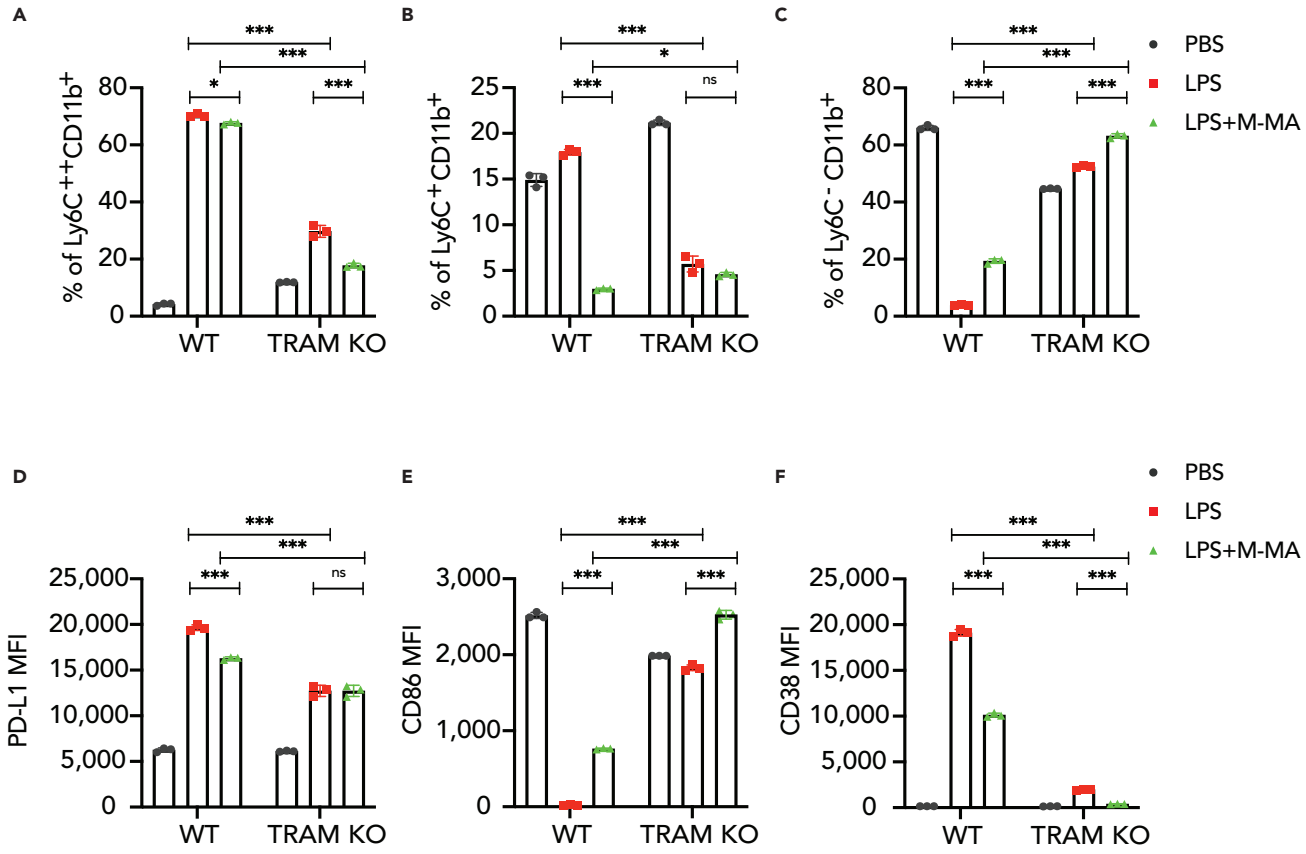

Figure 5. Additive effects of M-MA with TRAM deletion in restoring monocyte homeostasis

M-CSF maintained BMDMs from WT or TRAM KO mice were treated with the same treatments as described above.

(A–C) The frequencies of Ly6C^{++} CD11b^{+}, Ly6C^{+} CD11b^{+} and Ly6C^{-} CD11b^{+} were quantified.

(D–F) The MFIs of PD-L1 (D), CD38 (E), and CD86 (F) in WT and TRAM KO monocytes were measured via flow cytometry. The data shown are representative of three independent biological replicates, and error bars indicate the means ± SD with n = 3 for each group. Statistical analysis was performed using two-way ANOVA, *p < 0.05, ***p < 0.001.

and suppression by M-MA (Figures 6B and 6J). Consequently, we observed a robust reduction of Akt in exhausted monocytes, and a partial restoration of Akt by M-MA (Figures 6B and 6K). Our data is consistent with independent studies reporting the restoration of Akt by immune-enhancing agents such as beta-glucan.[59] Collectively, our data reveal M-MA can potently restore the polarized signaling circuitry in exhausted monocytes (Figure 6C).

M-MA effectively re-balances the genomic methylation landscape of exhausted monocytes

Given the emerging appreciation of epigenetic alterations as the underlying mechanism for innate immune memory,[60–62] we next tested whether M-MA restores epigenetic homeostasis in exhausted monocytes. We analyzed genome-wide DNA methylation levels in cultured monocytes using an Infinium Mouse Methylation BeadChip arrays to profile changes in 5-methylcytosine (5mC) at CpG islands, gene promoters and enhancers, and additional sites of regulatory significance. Exhausted monocytes exhibited a significant increase in global DNA methylation levels that is partially restored by M-MA treatment (Mood's median test = 1.55 x 10^{-13}) (Figures 7A and 7B). Principal components and phylogenetic analysis different culture conditions revealed distinct patterns for PBS control, LPS, and LPS+MA cultured cells (Figures 7A and 7C). In total, we identified 12,034 hypermethylated and 4,108 hypomethylated CpG probes, most of which were shared between the LPS and LPS+MA conditions (Figures 7D and 7E, and Table S1). Based on chromatin state discovery and characterization (chromHMM) analysis, many of these changes were observed at gene enhancers and transcription start site flanking regions, suggesting their differential methylation is of regulatory significance (Figure S2A and Table S2).

Focusing on specific DMRs, we validated by BisPCR^{2} sequencing that DNA methylation at the *Plac8* promoter is fully rescued by M-MA treatment (Figure 7F). Gene ontology (GO) analysis of DMR nearest-linked genes revealed an enrichment of terms "oxidative phosphorylation" and "electron transport chain" specifically in M-MA-treated cells, highlighting the potential impact of M-MA on restoring metabolic homeostasis, as well as "adipogenesis", "TNF signaling", and "MAPK signaling" terms shared with cells treated with LPS alone (Table S3). Taken

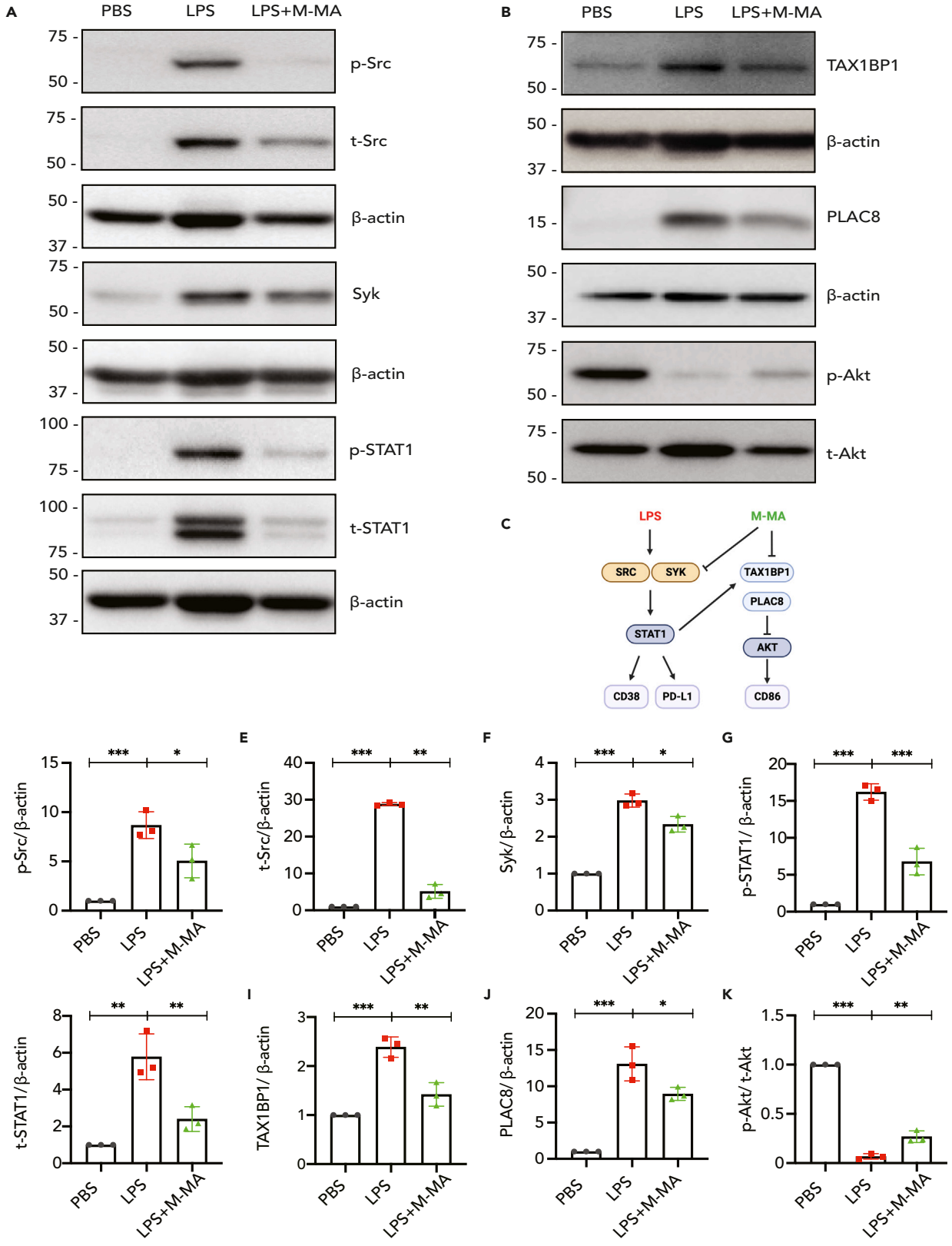
A
PBS
LPS
LPS+M-MA
p-Src
t-Src
β-actin
Syk
β-actin
p-STAT1
t-STAT1
β-actin
B
PBS
LPS
LPS+M-MA
TAX1BP1
β-actin
PLAC8
β-actin
p-Akt
t-Akt
C
LPS
M-MA
SRC
SYK
TAX1BP1
PLAC8
STAT1
AKT
CD38
PD-L1
CD86
D
p-Src/β-actin
E
t-Src/β-actin
F
Syk/β-actin
G
p-STAT1/ β-actin
H
t-STAT1/β-actin
I
TAX1BP1/ β-actin
J
PLAC8/ β-actin
K
p-Akt/ t-Akt
PBS
LPS
LPS+M-MA

Figure 6. M-MA potently blocks key signaling circuitry involved in monocyte exhaustion

M-CSF maintained BMDMs were treated PBS, high dose LPS (100 ng/mL), or high dose LPS plus M-MA (10 μg/mL) for 5 days. Monocytes were collected for western Blot. The levels of *p*-Src, t-Src, Syk, p-STAT, t-STAT1 (A) and TAX1BP1, PLAC8, *p*-Akt, t-Akt (B) were determined by western blot.

(C) Schematic illustration summarizing the possible mechanisms implicated in the prevention of monocyte exhaustion by M-MA blockade. The relative levels of *p*-Src (D), t-Src (E), Syk (F), p-STAT1 (G), t-STAT1 (H), TAX1BP1 (I), and PLAC8 (J) were normalized to β-actin. The relative level of *p*-AKT (K) was normalized to t-Akt. The data are representative of three independent biological replicates, and error bars represent means ± SD. *p < 0.05, **p < 0.01, ***p < 0.001, one-way ANOVA.

together, our data suggest that the exhaustion memory is imprinted at the level of DNA methylation, and this stable imprint can be effectively reversed by co-treatment with M-MA.

DISCUSSION

Our current study characterizes M-MA as a potential agent in relieving monocyte exhaustion based on the following observations. First, M-MA potently reduces the expression of pathogenic inflammatory mediator CD38 and immune suppressor PD-L1, as well as restores the expression of immune enhancer CD86. Second, M-MA restores mitochondria function and monocyte's capability in supporting T cell proliferation. Third, M-MA attenuates pathogenic inflammatory signaling circuitry through reducing Src family kinase-mediated activation of STAT1 and restores immune-enhancing Akt activation through blocking STAT1-mediated expression of molecular suppressors such as PLAC8 and TAX1BP1. Fourth, M-MA can potently erase epigenetic memory at the level of DNA methylation.

Our data complement emerging basic and clinical studies that reveal conceptual as well as clinical significance of "trained" innate immunity related to the potential protection against polymicrobial-induced sepsis. Selected microbes such as BCG as well as microbial components including fungal products beta-glucan were shown to "train" innate monocytes into a memory state with elevated expression of immune-enhancing mediators.[63,64] Clinical trials based on the concept of trained innate immunity are emerging with the objective of developing innate-based vaccines in offering broad-spectrum protection against diverse infectious agents including SARS-CoV-2.[65,66] The experimental model of "trained" immunity relies upon the two-hit approach, with the first hit with immune-enhancing agents enabling innate cells to have a more robust immune response to a secondary challenge.[67] Despite its translational potential in the development of innate-based preventative vaccines, this approach is not amenable to addressing the progression of immune exhaustion after the onset of sepsis. Patients recovering from sepsis or severe COVID-19 often exhibit chronic complications with lingering morbidity and mortality risks.[68,69] Analogous to T cell exhaustion which can develop following repetitive and prolonged challenges, monocytes exposed to prolonged septic signals develop a chronic exhausted state, characterized by reduced differentiation as well as pathogenic inflammatory and immune suppressive features.[9,70] Monocyte exhaustion can be observed in human and murine sepsis,[10,71,72] and can be generated *in vitro* through prolonged treatment with bacterial endotoxin LPS.[9,73]

The persistence of exhausted monocytes compromises host's immune defense and aggravates pathological tissue damage, leading to elevated sepsis mortality/morbidity. Despite its vital clinical relevance, efforts in alleviating monocyte exhaustion due to prolonged challenges were limited, and our current study fills this critical gap in knowledge. Our data demonstrate the potency of methoxy-MA in effectively attenuating monocyte exhaustion generated by prolonged LPS challenge. We validate that exhausted monocytes due to repetitive and prolonged LPS treatment exhibit not only key molecular signatures reported in sepsis (e.g., elevated CD38, PD-L1, and reduced CD86),[74] but also functional signatures of exhaustion (e.g., compromised mitochondria function, potent suppression of T cell proliferation and activation). Our data further demonstrate that M-MA co-treatment may alleviate the development of monocyte exhaustion, at molecular and functional levels. Our study complements existing studies in the area of innate training and suggests potential strategies in alleviating monocyte exhaustion.

Mechanistically, our current study reveals several less-appreciated principles for the generation and alleviation of monocyte exhaustion. It is well-known that the responses of naive cells to initial LPS challenge involve the activation of multiple signaling pathways and transcription factors that include NFkB and IRFs,[73,75] leading to the pleiotropic expression of genes ranging from pro- and anti-inflammatory mediators; immune-enhancers as well as suppressors.[73,76] Independent reports reveal that the TLR4 adaptor TRAM serves as the most critical node essential for the generic cellular response to LPS ranging from NFkB as well as IRFs.[47,77] Following the initial phase of pleiotropic responses, LPS-treated cells exhibit a second phase of "tolerance", as reflected in a generic suppression of pro-inflammatory cytokines, interferon-related genes and immune-enhancing mediators.[73,76] During the second phase of tolerance, both NFkB and IRF signaling pathways are suppressed.[73,75] Intriguingly, exhausted monocytes with repetitive and prolonged LPS challenges are not only tolerant with reduced NFkB and IRF signaling,[75] but also preferentially retain robust induction and activation of STAT1 protein.[9] We validated that both the total and phosphorylated levels of Src family kinases (SFKs) such as Syk and Src are highly elevated in exhausted monocytes following 5-day culture. Sustained induction of SFKs can contribute to the activation loop involving the induction as well as phosphorylation of STAT1 which further sustains the induction of pathogenic inflammatory mediators such as CD38 in exhausted monocytes. We confirmed the increased levels of total as well as phosphorylated STAT1, Syk, and Src in exhausted monocytes, and demonstrated a robust reduction of these key signaling mediators in monocytes co-treated with M-MA. Our mechanistic studies are consistent with a previous study showing that deletion of STAT1 can potently protect experimental animals in developing severe sepsis.[51] STAT1 not only drives the expression of inflammatory mediators but may also induce the expression of immune suppressors such as PLAC8 and TAX1BP1. Both TAX1BP1 and PLAC8 are shown to cause immune suppression by inhibiting TBK1.[54,55] TBK1 activation is important for Akt and NFkB-mediated expression of immune-enhancing genes such as CD86. Consistent with our protein analyses, our methylation data reveal the differential methylation of *Plac8* in exhausted monocytes and its restoration by M-MA.

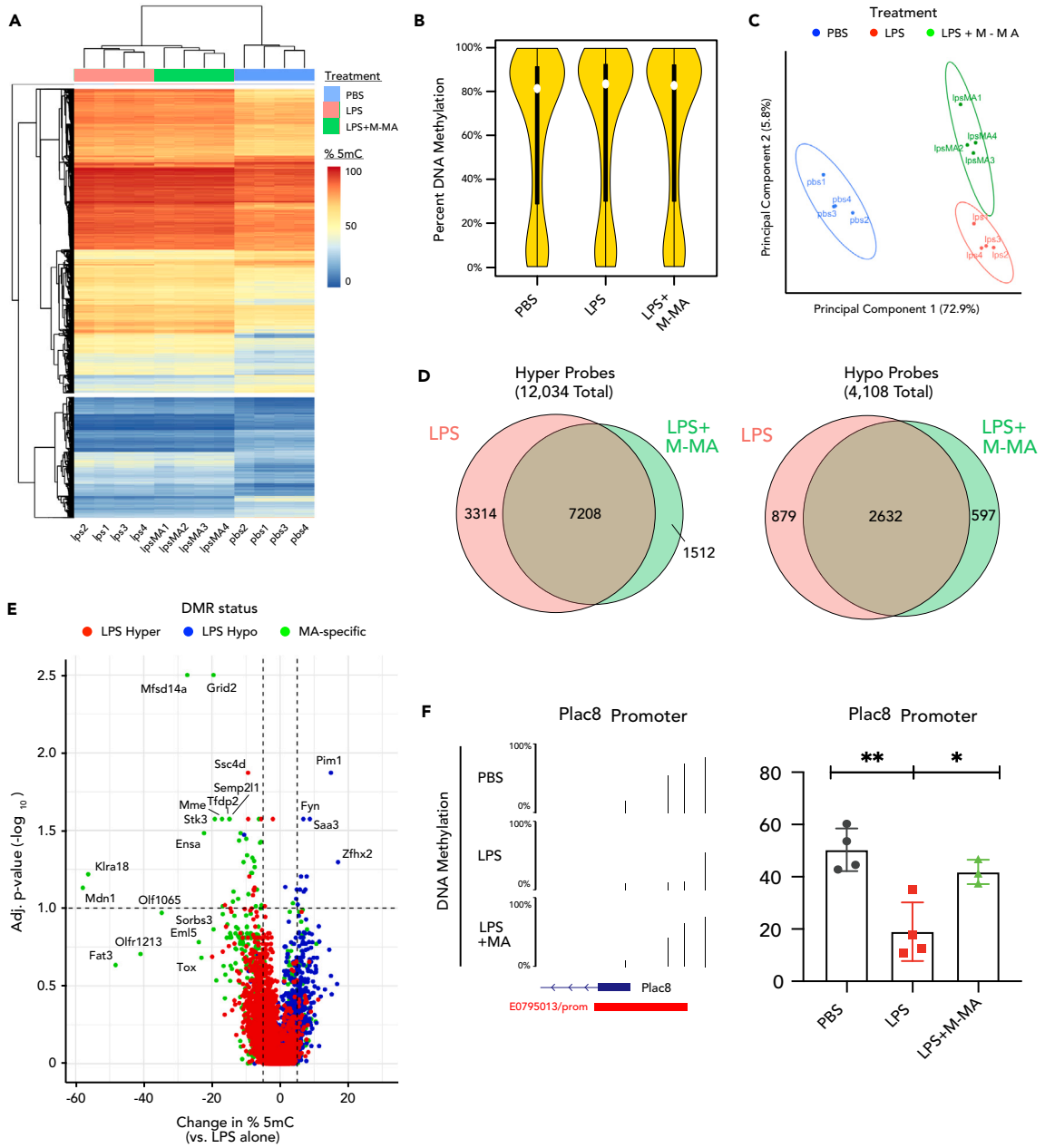

Figure 7. M-MA effectively re-balances the genomic methylation landscape of exhausted monocytes

(A) Correlation heatmap for DNA methylation at differentially methylated CpG probes following 5 days of PBS control or repetitive LPS stimulation in the presence or absence of M-MA (≥5% difference in % 5mC vs. PBS control; FDR <5%; n = 4 for each treatment).

(B) Violin plots of average DNA methylation levels at each probe CpG for the BMMCs under PBS control or repetitive-LPS stimulation +/− M-MA treatment, with boxplots indicating medians, interquartile ranges, and 95% confidence intervals (n = 4 for each condition).

(C) Principal component analysis of differentially methylated CpG probes in PBS control- (blue), LPS- (red), or LPS+M-MA-treated (green) BMMCs. Ovals indicate the normal distribution for each treatment.

(D) Venn diagrams for differentially methylated CpG probes in cells treated with LPS alone (red) or LPS + M-MA (green).

(E) Volcano plot for altered DNA methylation at DMRs in LPS+M-MA-treated BMMCs versus treatment with LPS alone. Probes are colored based on observed differential methylation patterns in LPS-treated cells relative to PBS control (red: hypermethylated; blue: hypomethylated) or probes that exhibit differential methylation only in LPS+M-MA cells (green). Dotted lines indicate the change in DNA methylation (+/− 5%) and adjusted p value (<0.1) cut-offs for DMRs. Nearest linked genes for select DMRs are indicated.

(F) UCSC browser track views (left) and mean DNA methylation levels (right) of MiSeq-validated DMRs at the Plac8 promoter (chr5:100,570,157-100,573,097) regions for PBS control, LPS, or LPS+M-MA-treated BMMCs. ENCODE annotated promoters (red) are depicted in the bottom track. Bar graphs represent means ± standard deviation (SD) with n = 4 for each group. Statistical analysis was performed using one-way ANOVA, *p < 0.05, **p < 0.01.

Previous studies regarding the related concept of innate priming or tolerance primarily focused on epigenetic changes caused by histone modifications.[62,78] However, emerging studies suggest that histone-related chromatin modifications may be transient, whereas we have recently demonstrated broad changes in the DNA methylome of exhausted cells.[79,80] Our data reveal profound changes in genome-wide DNA methylation patterns in exhausted monocytes (Figure 7). Massive genome-wide methylation correlated with global gene suppression of most cytokines and IFN related genes reported in endotoxin tolerance,[76] and reflected in our previously published scRNA-seq dataset.[9] We also independently validated through targeted RT-PCR assay that IFNβ and IFNAR were not induced in exhausted monocytes (Figure S3). However, despite the global increase in DNA methylation related to tolerance, we validated the selective hypo-methylation of Plac8, allowing the selective induction of PLAC8 mediated by STAT1.

We also observed systemic alterations in methylated genes involved in metabolisms, consistent with an independent *in vivo* study reporting compromised mitochondria metabolism and bioenergetic failure in exhausted human monocytes isolated from septic patients with liver failure.[81] Together, our integrated signaling studies and genome-wide methylation analyses reveal key molecular signatures of monocyte exhaustion, as well as potencies of M-MA in restoring monocyte homeostasis.

Limitations of the study

Despite the promising phenotype of M-MA in restoring monocyte homeostasis, it is yet to be determined regarding how M-MA exerts its beneficial functions. Although a previous *Nature Communications* report suggests that all forms of free mycolic acid share the TREM2 receptor in mediating cellular responses,[42] our data reveal that the restoration effects of M-MA on exhausted monocytes are independent of TREM2. Other scavenger receptors such as Mincle should be tested in future studies.[82] The fact that the branched M-MA has better efficacy than the non-branched alpha-mycolic acid suggests that M-MA may generically relieve cell membrane lipid-raft stress and reduce exhaustion signaling, in a receptor independent fashion. This might be a rudimentary principle of innate cell regulation independent of cellular receptors. Key innate signaling adaptors and mediators such as TRAM and SRC kinase are known to be covalently conjugated with lipids,[47,83] enabling their intercalation within membrane rafts. Activation of lipid raft mediated by TRAM may then be generically responsible for innate immune activation dynamics. This receptor independent as well as dependent processes need to be carefully addressed in future studies in order to fully understand the underlying mechanisms.

Our observation holds conceptual relevance in modulating innate immune memory through M-MA, which resonates with emerging clinical interests of "trained innate immunity" in potentially mitigating sepsis severity as well as other diseases.[84,85] Despite these promising advances in the general area of innate immune memory, the complex *in vivo* modulations of immune environments during the early and late courses of sepsis still remain poorly understood. Immune and/or inflammatory dysregulation during sepsis likely involves a wide array of immune cells and tissues with complex adaptation dynamics during distinct phases of sepsis pathogenesis. Our current study serves as an initial attempt in addressing one unique aspect of innate memory modulation related to monocyte exhaustion, which may assist future *in vivo* studies aimed at better harnessing the efficacies of innate memory training in managing monocyte exhaustion during various stages of sepsis pathogenesis. The pharmacodynamics and pharmacokinetics of M-MA and related BCG compounds should be carefully examined in animal models, in order to better evaluate the proper window of intervention as well as side effects.

STAR★METHODS

Detailed methods are provided in the online version of this paper and include the following:

- KEY RESOURCES TABLE
- RESOURCE AVAILABILITY
  - Lead contact
  - Materials availability
  - Data and code availability
- EXPERIMENTAL MODEL AND STUDY PARTICIPANT DETAILS
  - Animals and ethics statement
- METHOD DETAILS
  - Murine primary monocyte isolation and culture
  - Human monocyte culture
  - T Cell Isolation and coculture
  - NAD and lactate assay
  - Western blot
  - Flow cytometry
  - Quantitative RT-PCR
  - Infinium Mouse Methylation BeadChip array
  - Bisulfite next-generation sequencing
  - Infinium BeadChip array analysis
  - BisPCR2 sequencing analysis
- QUANTIFICATION AND STATISTICAL ANALYSIS

SUPPLEMENTAL INFORMATION

Supplemental information can be found online at https://doi.org/10.1016/j.isci.2024.108978.

ACKNOWLEDGMENTS

This study was supported in part through grants from NIH R01 AI172133 to L.L, NIH 5TL1DK132771 to B.C, and American Heart Association Postdoctoral Fellowship Award 23POST1027469 to J.W. We appreciate that technical assistance from the staff member of Li Laboratory including Feng Xu. Images were made using BioRender.

AUTHOR CONTRIBUTIONS

Y.W. designed the studies; performed experiments; analyzed the data; and drafted the manuscript. B.C., J.W., and Y.Z. conducted experiments, analyzed the data and wrote the manuscript. L.L. designed, supervised the studies, and wrote the manuscript.

DECLARATION OF INTERESTS

The authors declare no competing interests.

Received: September 15, 2023
Revised: November 27, 2023
Accepted: January 16, 2024
Published: January 19, 2024

REFERENCES

1. CDC (2020). Sepsis. https://www.who.int/news-room/fact-sheets/detail/sepsis.
2. Hotchkiss, R.S., Monneret, G., and Payen, D. (2013). Sepsis-induced immunosuppression: from cellular dysfunctions to immunotherapy. Nat. Rev. Immunol. *13*, 862–874. https://doi.org/10.1038/nri3552.
3. Angus, D.C., and van der Poll, T. (2013). Severe sepsis and septic shock. N. Engl. J. Med. *369*, 840–851. https://doi.org/10.1056/NEJMra1208623.
4. Wiersinga, W.J., Leopold, S.J., Cranendonk, D.R., and van Der Poll, T. (2014). Host innate immune responses to sepsis. Virulence *5*, 36–44. https://doi.org/10.4161/viru.25436.
5. Baudesson de Chanville, C., Chousterman, B.G., Hamon, P., Laviron, M., Guillou, N., Loyher, P.L., Meghraoui-Kheddar, A., Barthelemy, S., Deterre, P., Boissonnas, A., and Combadière, C. (2020). Sepsis triggers a late expansion of functionally impaired tissue-vascular inflammatory monocytes during clinical recovery. Front. Immunol. *11*, 675. https://doi.org/10.3389/fimmu.2020.00675.
6. Hotchkiss, R.S., Monneret, G., and Payen, D. (2013). Immunosuppression in sepsis: a novel understanding of the disorder and a new therapeutic approach. Lancet Infect. Dis. *13*, 260–268. https://doi.org/10.1016/s1473-3099(13)70001-x.
7. Bomans, K., Schenz, J., Sztwiertnia, I., Schaack, D., Weigand, M.A., and Uhle, F. (2018). Sepsis induces a long-lasting state of trained immunity in bone marrow monocytes. Front. Immunol. *9*, 2685. https://doi.org/10.3389/fimmu.2018.02685.
8. Naler, L.B., Hsieh, Y.-P., Geng, S., Zhou, Z., Li, L., and Lu, C. (2022). Epigenomic and transcriptomic analyses reveal differences between low-grade inflammation and severe exhaustion in LPS-challenged murine monocytes. Commun. Biol. *5*, 102. https://doi.org/10.1038/s42003-022-03035-2.
9. Pradhan, K., Yi, Z., Geng, S., and Li, L. (2021). Development of exhausted memory monocytes and underlying mechanisms. Front. Immunol. *12*, 778830. https://doi.org/10.3389/fimmu.2021.778830.
10. Ferreira da Mota, N.V., Brunialti, M.K.C., Santos, S.S., Machado, F.R., Assuncao, M., Azevedo, L.C.P., and Salomao, R. (2018). Immunophenotyping of monocytes during human sepsis shows impairment in antigen presentation: a shift toward nonclassical differentiation and upregulation of FCγRi-receptor. Shock *50*, 293–300. https://doi.org/10.1097/SHK.0000000000001078.
11. Patil, N.K., Guo, Y., Luan, L., and Sherwood, E.R. (2017). Targeting immune cell checkpoints during sepsis. Int. J. Mol. Sci. *18*, 2413. https://doi.org/10.3390/ijms18112413.
12. Hogan, K.A., Chini, C.C.S., and Chini, E.N. (2019). The multi-faceted ecto-enzyme CD38: roles in immunomodulation, cancer, aging, and metabolic diseases. Front. Immunol. *10*, 1187. https://doi.org/10.3389/fimmu.2019.01187.
13. Aksoy, P., White, T.A., Thompson, M., and Chini, E.N. (2006). Regulation of intracellular levels of NAD: a novel role for CD38. Biochem. Biophys. Res. Commun. *345*, 1386–1392. https://doi.org/10.2174/138161209787185788.
14. Camacho-Pereira, J., Tarragó, M.G., Chini, C.C.S., Nin, V., Escande, C., Warner, G.M., Puranik, A.S., Schoon, R.A., Reid, J.M., Galina, A., and Chini, E.N. (2016). CD38 dictates age-related NAD decline and mitochondrial dysfunction through an SIRT3-dependent mechanism. Cell Metabol. *23*, 1127–1139. https://doi.org/10.1016/j.cmet.2016.05.006.
15. Covarrubias, A.J., Perrone, R., Grozio, A., and Verdin, E. (2021). NAD+ metabolism and its roles in cellular processes during ageing. Nat. Rev. Mol. Cell Biol. *22*, 119–141. https://doi.org/10.1038/s41580-020-00313-x.
16. Fan, L., Cacicedo, J.M., and Ido, Y. (2020). Impaired nicotinamide adenine dinucleotide (NAD+) metabolism in diabetes and diabetic tissues: Implications for nicotinamide-related compound treatment. J. Diabetes Investig. *11*, 1403–1419. https://doi.org/10.1111/jdi.13303.
17. Hong, G., Zheng, D., Zhang, L., Ni, R., Wang, G., Fan, G.-C., Lu, Z., and Peng, T. (2018). Administration of nicotinamide riboside prevents oxidative stress and organ injury in sepsis. Free Radic. Biol. Med. *123*, 125–137. https://doi.org/10.1016/j.freeradbiomed.2018.05.073.
18. Miller, R., Wentzel, A.R., and Richards, G.A. (2020). COVID-19: NAD+ deficiency may predispose the aged, obese and type2 diabetics to mortality through its effect on SIRT1 activity. Med. Hypotheses *144*, 110044. https://doi.org/10.1016/j.mehy.2020.110044.
19. Zhang, Y., Zhou, Y., Lou, J., Li, J., Bo, L., Zhu, K., Wan, X., Deng, X., and Cai, Z. (2010). PD-L1 blockade improves survival in experimental sepsis by inhibiting lymphocyte apoptosis and reversing monocyte dysfunction. Crit. Care *14*, R220–R229. https://doi.org/10.1186/cc9354.
20. Zitvogel, L., and Kroemer, G. (2012). Targeting PD-1/PD-L1 interactions for cancer immunotherapy. OncoImmunology *1*, 1223–1225.
21. Thomas, G.D., Hamers, A.A.J., Nakao, C., Marcovecchio, P., Taylor, A.M., McSkimming, C., Nguyen, A.T., McNamara, C.A., and Hedrick, C.C. (2017). Human blood monocyte subsets: a new gating strategy defined using cell surface markers identified by mass cytometry. Arterioscler. Thromb. Vasc. Biol. *37*, 1548–1558. https://doi.org/10.1161/ATVBAHA.117.309145.
22. Matsuo, K., and Yasutomi, Y. (2011). Mycobacterium bovis Bacille Calmette-Guérin as a Vaccine Vector for Global Infectious Disease Control. Tuberc. Res. Treat. *2011*, 574591. https://doi.org/10.1155/2011/574591.
23. Escobar, L.E., Molina-Cruz, A., and Barillas-Mury, C. (2020). BCG vaccine protection from severe coronavirus disease 2019 (COVID-19). Proc. Natl. Acad. Sci. USA *117*, 17720–17726. https://doi.org/10.1073/pnas.2008410117.
24. Aspatwar, A., Gong, W., Wang, S., Wu, X., and Parkkila, S. (2022). Tuberculosis vaccine BCG: the magical effect of the old vaccine in

the fight against the COVID-19 pandemic. Int. Rev. Immunol. *41*, 283–296. https://doi.org/10.1080/08830185.2021.1922685.

25. Covián, C., Fernández-Fierro, A., Retamal-Díaz, A., Díaz, F.E., Vasquez, A.E., Lay, M.K., Riedel, C.A., González, P.A., Bueno, S.M., and Kalergis, A.M. (2019). BCG-Induced Cross-Protection and Development of Trained Immunity: Implication for Vaccine Design. Front. Immunol. *10*, 2806. https://doi.org/10.3389/fimmu.2019.02806.
26. Moerings, B.G.J., de Graaff, P., Furber, M., Witkamp, R.F., Debets, R., Mes, J.J., van Bergenhenegouwen, J., and Govers, C. (2021). Continuous Exposure to Non-Soluble β-Glucans Induces Trained Immunity in M-CSF-Differentiated Macrophages. Front. Immunol. *12*, 672796. https://doi.org/10.3389/fimmu.2021.672796.
27. Ishikawa, E., Ishikawa, T., Morita, Y.S., Toyonaga, K., Yamada, H., Takeuchi, O., Kinoshita, T., Akira, S., Yoshikai, Y., and Yamasaki, S. (2009). Direct recognition of the mycobacterial glycolipid, trehalose dimycolate, by C-type lectin Mincle. J. Exp. Med. *206*, 2879–2888. https://doi.org/10.1084/jem.20091750.
28. Petrovsky, N., and Cooper, P.D. (2011). Carbohydrate-based immune adjuvants. Expert Rev. Vaccines *10*, 523–537. https://doi.org/10.1586/erv.11.30.
29. Kleinnijenhuis, J., Quintin, J., Preijers, F., Joosten, L.A.B., Ifrim, D.C., Saeed, S., Jacobs, C., van Loenhout, J., de Jong, D., Stunnenberg, H.G., et al. (2012). Bacille Calmette-Guerin induces NOD2-dependent nonspecific protection from reinfection via epigenetic reprogramming of monocytes. Proc. Natl. Acad. Sci. USA *109*, 17537–17542. https://doi.org/10.1073/pnas.1202870109.
30. Masihi, K.N., Brehmer, W., Lange, W., Werner, H., and Ribi, E. (1985). Trehalose dimycolate from various mycobacterial species induces differing anti-infectious activities in combination with muramyl dipeptide. Infect. Immun. *50*, 938–940. https://doi.org/10.1128/iai.50.3.938-940.1985.
31. Geng, S., Zhang, Y., Yi, Z., Lu, R., and Li, L. (2021). Resolving monocytes generated through TRAM deletion attenuate atherosclerosis. JCI Insight *6*, e149651. https://doi.org/10.1172/jci.insight.149651.
32. Nasser, H., Adhikary, P., Abdel-Daim, A., Noyori, O., Panaampon, J., Kariya, R., Okada, S., Ma, W., Baba, M., Takizawa, H., et al. (2020). Establishment of bone marrow-derived M-CSF receptor-dependent self-renewing macrophages. Cell Death Dis. *6*, 63. https://doi.org/10.1038/s41420-020-00300-3.
33. Subramanian, S., Busch, C.J.L., Molawi, K., Geirsdottir, L., Maurizio, J., Vargas Aguilar, S., Belahbib, H., Gimenez, G., Yuda, R.A.A., Burkon, M., et al. (2022). Long-term culture-expanded alveolar macrophages restore their full epigenetic identity after transfer *in vivo*. Nat. Immunol. *23*, 458–468. https://doi.org/10.1038/s41590-022-01146-w.
34. Rahtes, A., Pradhan, K., Sarma, M., Xie, D., Lu, C., and Li, L. (2020). Phenylbutyrate facilitates homeostasis of non-resolving inflammatory macrophages. Innate Immun. *26*, 62–72. https://doi.org/10.1177/1753425919879503.
35. Chousterman, B.G., Boissonnas, A., Poupel, L., Baudesson de Chanville, C., Adam, J., Tabibzadeh, N., Licata, F., Lukaszewicz, A.C., Lombès, A., Deterre, P., et al. (2016). Ly6Chigh Monocytes Protect against Kidney Damage during Sepsis via a CX3CR1-Dependent Adhesion Mechanism. J. Am. Soc. Nephrol. *27*, 792–803. https://doi.org/10.1681/asn.2015010009.
36. Stein, L.R., and Imai, S.-I. (2012). The dynamic regulation of NAD metabolism in mitochondria. Trends Endocrinol. Metabol. *23*, 420–428. https://doi.org/10.1016/j.tem.2012.06.005.
37. Tran, M.T., Zsengeller, Z.K., Berg, A.H., Khankin, E.V., Bhasin, M.K., Kim, W., Clish, C.B., Stillman, I.E., Karumanchi, S.A., Rhee, E.P., and Parikh, S.M. (2016). PGC1α drives NAD biosynthesis linking oxidative metabolism to renal protection. Nature *531*, 528–532. https://doi.org/10.1038/nature17184.
38. Rius-Pérez, S., Torres-Cuevas, I., Millán, I., Ortega, Á.L., and Pérez, S. (2020). PGC-1α, inflammation, and oxidative stress: an integrative view in metabolism. Oxid. Med. Cell. Longev. *2020*, 1452696. https://doi.org/10.1155/2020/1452696.
39. Bryn, T., Yaqub, S., Mahic, M., Henjum, K., Aandahl, E.M., and Taskén, K. (2008). LPS-activated monocytes suppress T-cell immune responses and induce FOXP3+ T cells through a COX-2–PGE2-dependent mechanism. Int. Immunol. *20*, 235–245. https://doi.org/10.1093/intimm/dxm134.
40. Subauste, C.S., de Waal Malefyt, R., and Fuh, F. (1998). Role of CD80 (B7. 1) and CD86 (B7. 2) in the immune response to an intracellular pathogen. J. Immunol. *160*, 1831–1840. https://doi.org/10.4049/jimmunol.160.4.1831.
41. Kuang, D.-M., Zhao, Q., Peng, C., Xu, J., Zhang, J.-P., Wu, C., and Zheng, L. (2009). Activated monocytes in peritumoral stroma of hepatocellular carcinoma foster immune privilege and disease progression through PD-L1. J. Exp. Med. *206*, 1327–1337. https://doi.org/10.1084/jem.20082173.
42. Iizasa, E., Chuma, Y., Uematsu, T., Kubota, M., Kawaguchi, H., Umemura, M., Toyonaga, K., Kiyohara, H., Yano, I., Colonna, M., et al. (2021). TREM2 is a receptor for non-glycosylated mycolic acids of mycobacteria that limits anti-mycobacterial macrophage activation. Nat. Commun. *12*, 2299. https://doi.org/10.1038/s41467-021-22620-3.
43. Gay, N.J., Symmons, M.F., Gangloff, M., and Bryant, C.E. (2014). Assembly and localization of Toll-like receptor signalling complexes. Nat. Rev. Immunol. *14*, 546–558. https://doi.org/10.1038/nri3713.
44. Guven-Maiorov, E., Keskin, O., Gursoy, A., VanWaes, C., Chen, Z., Tsai, C.-J., and Nussinov, R. (2015). The architecture of the TIR domain signalosome in the Toll-like receptor-4 signaling pathway. Sci. Rep. *5*, 13128. https://doi.org/10.1038/srep13128.
45. Korade, Z., and Kenworthy, A.K. (2008). Lipid rafts, cholesterol, and the brain. Neuropharmacology *55*, 1265–1273. https://doi.org/10.1016/j.neuropharm.2008.02.019.
46. Mercier, R., Domínguez-Cuevas, P., and Errington, J. (2012). Crucial role for membrane fluidity in proliferation of primitive cells. Cell Rep. *1*, 417–423. https://doi.org/10.1016/j.celrep.2012.03.008.
47. Rowe, D.C., McGettrick, A.F., Latz, E., Monks, B.G., Gay, N.J., Yamamoto, M., Akira, S., O'Neill, L.A., Fitzgerald, K.A., and Golenbock, D.T. (2006). The myristoylation of TRIF-related adaptor molecule is essential for Toll-like receptor 4 signal transduction. Proc. Natl. Acad. Sci. USA *103*, 6299–6304. https://doi.org/10.1073/pnas.0510041103.
48. Qing, Y., and Stark, G.R. (2004). Alternative activation of STAT1 and STAT3 in response to interferon-γ. J. Biol. Chem. *279*, 41679–41685. https://doi.org/10.1074/jbc.M406413200.
49. Costa, F., Marchica, V., Storti, P., Malavasi, F., and Giuliani, N. (2021). PD-L1/PD-1 Axis in Multiple Myeloma Microenvironment and a Possible Link with CD38-Mediated Immune-Suppression. Cancers *13*, 164. https://doi.org/10.3390/cancers13020164.
50. Ogiya, D., Liu, J., Ohguchi, H., Kurata, K., Samur, M.K., Tai, Y.-T., Adamia, S., Ando, K., Hideshima, T., and Anderson, K.C. (2020). The JAK-STAT pathway regulates CD38 on myeloma cells in the bone marrow microenvironment: Therapeutic implications. Blood *136*, 2334–2345. https://doi.org/10.1182/blood.2019004332.
51. Herzig, D., Fang, G., Toliver-Kinsky, T.E., Guo, Y., Bohannon, J., and Sherwood, E.R. (2012). STAT1-deficient mice are resistant to cecal ligation and puncture-induced septic shock. Shock *38*, 395–402. https://doi.org/10.1097/SHK.0b013e318265a2ab.
52. Wang, A., Kang, X., Wang, J., and Zhang, S. (2023). IFIH1/IRF1/STAT1 promotes sepsis associated inflammatory lung injury via activating macrophage M1 polarization. Int. Immunopharm. *114*, 109478. https://doi.org/10.1016/j.intimp.2022.109478.
53. Tirpude, N.V., Sharma, A., Joshi, R., Kumari, M., and Acharya, V. (2021). Vitex negundo Linn. extract alleviates inflammatory aggravation and lung injury by modulating AMPK/PI3K/Akt/p38-NF-κB and TGF-β/Smad/Bcl2/caspase/LC3 cascade and macrophages activation in murine model of OVA-LPS induced allergic asthma. J. Ethnopharmacol. *271*, 113894. https://doi.org/10.1016/j.jep.2021.113894.
54. Parvatiyar, K., Barber, G.N., and Harhaj, E.W. (2010). TAX1BP1 and A20 inhibit antiviral signaling by targeting TBK1-IKKi kinases. J. Biol. Chem. *285*, 14999–15009. https://doi.org/10.1074/jbc.M110.109819.
55. Zhang, Y., Cen, J., Yuan, G., Jia, Z., Chen, K., Gao, W., Chen, J., Adamek, M., Jia, Z., and Zou, J. (2023). DDX5 inhibits type I IFN production by promoting degradation of TBK1 and disrupting formation of TBK1 – TRAF3 complex. Cell. Mol. Life Sci. *80*, 212. https://doi.org/10.1007/s00018-023-04860-2.
56. Banerjee, S., Mohammed, A., Wong, H.R., Palaniyar, N., and Kamaleswaran, R. (2021). Machine Learning Identifies Complicated Sepsis Course and Subsequent Mortality Based on 20 Genes in Peripheral Blood Immune Cells at 24 H Post-ICU Admission. Front. Immunol. *12*, 592303. https://doi.org/10.3389/fimmu.2021.592303.
57. Reyes, M., Filbin, M.R., Bhattacharyya, R.P., Billman, K., Eisenhaure, T., Hung, D.T., Levy, B.D., Baron, R.M., Blainey, P.C., Goldberg, M.B., and Hacohen, N. (2020). An immune-cell signature of bacterial sepsis. Nat. Med. *26*, 333–340. https://doi.org/10.1038/s41591-020-0752-4.
58. Zhang, K., Wang, Y., Chen, S., Mao, J., Jin, Y., Ye, H., Zhang, Y., Liu, X., Gong, C., Cheng, X., et al. (2023). TREM2hi resident macrophages protect the septic heart by maintaining cardiomyocyte homeostasis. Nat. Metab. *5*, 129–146. https://doi.org/10.1038/s42255-022-00715-5.
59. Hsu, M.J., Lee, S.S., and Lin, W.W. (2002). Polysaccharide purified from Ganoderma lucidum inhibits spontaneous and Fas-mediated apoptosis in human neutrophils

through activation of the phosphatidylinositol 3 kinase/Akt signaling pathway. J. Leukoc. Biol. *72*, 207–216. https://doi.org/10.1189/jlb.72.1.207.

60. Italiani, P., Della Camera, G., and Boraschi, D. (2020). Induction of innate immune memory by engineered nanoparticles in monocytes/macrophages: From hypothesis to reality. Front. Immunol. *11*, 566309. https://doi.org/10.3389/fimmu.2020.566309.
61. Sun, S., and Barreiro, L.B. (2020). The epigenetically-encoded memory of the innate immune system. Curr. Opin. Immunol. *65*, 7–13. https://doi.org/10.1016/j.coi.2020.02.002.
62. van der Heijden, C.D.C.C., Noz, M.P., Joosten, L.A.B., Netea, M.G., Riksen, N.P., and Keating, S.T. (2018). Epigenetics and Trained Immunity. Antioxidants Redox Signal. *29*, 1023–1040. https://doi.org/10.1089/ars.2017.7310.
63. Arts, R.J.W., Carvalho, A., La Rocca, C., Palma, C., Rodrigues, F., Silvestre, R., Kleinnijenhuis, J., Lachmandas, E., Gonçalves, L.G., Belinha, A., et al. (2016). Immunometabolic Pathways in BCG-Induced Trained Immunity. Cell Rep. *17*, 2562–2571. https://doi.org/10.1016/j.celrep.2016.11.011.
64. Mourits, V.P., Wijkmans, J.C., Joosten, L.A., and Netea, M.G. (2018). Trained immunity as a novel therapeutic strategy. Curr. Opin. Pharmacol. *41*, 52–58. https://doi.org/10.1016/j.coph.2018.04.007.
65. Brueggeman, J.M., Zhao, J., Schank, M., Yao, Z.Q., and Moorman, J.P. (2022). Trained Immunity: An Overview and the Impact on COVID-19. Front. Immunol. *13*, 837524. https://doi.org/10.3389/fimmu.2022.837524.
66. Netea, M.G., Giamarellos-Bourboulis, E.J., Domínguez-Andrés, J., Curtis, N., van Crevel, R., van de Veerdonk, F.L., and Bonten, M. (2020). Trained Immunity: a Tool for Reducing Susceptibility to and the Severity of SARS-CoV-2 Infection. Cell *181*, 969–977. https://doi.org/10.1016/j.cell.2020.04.042.
67. Muenzer, J.T., Davis, C.G., Dunne, B.S., Unsinger, J., Dunne, W.M., and Hotchkiss, R.S. (2006). Pneumonia after cecal ligation and puncture: a clinically relevant "two-hit" model of sepsis. Shock *26*, 565–570. https://doi.org/10.1097/01.shk.0000235130.82363.ed.
68. Benjamim, C.F., Hogaboam, C.M., and Kunkel, S.L. (2004). The chronic consequences of severe sepsis. J. Leukoc. Biol. *75*, 408–412. https://doi.org/10.1189/jlb.0503214.
69. Booth, A., Reed, A.B., Ponzo, S., Yassaee, A., Aral, M., Plans, D., Labrique, A., and Mohan, D. (2021). Population risk factors for severe disease and mortality in COVID-19: A global systematic review and meta-analysis. PLoS One *16*, e0247461. https://doi.org/10.1371/journal.pone.0247461.
70. Yi, J.S., Cox, M.A., and Zajac, A.J. (2010). T-cell exhaustion: characteristics, causes and conversion. Immunology *129*, 474–481. https://doi.org/10.1111/j.1365-2567.2010.03255.x.
71. Hortová-Kohoutková, M., Lázničková, P., Bendíčková, K., De Zuani, M., Andrejčinová, I., Tomášková, V., Suk, P., Šrámek, V., Helán, M., and Frič, J. (2020). Differences in monocyte subsets are associated with short-term survival in patients with septic shock. J. Cell Mol. Med. *24*, 12504–12512. https://doi.org/10.1111/jcmm.15791.
72. Newton, S., Ding, Y., Chung, C.S., Chen, Y., Lomas-Neira, J.L., and Ayala, A. (2004). Sepsis-induced changes in macrophage co-stimulatory molecule expression: CD86 as a regulator of anti-inflammatory IL-10 response. Surg. Infect. *5*, 375–383. https://doi.org/10.1089/sur.2004.5.375.
73. Morris, M.C., Gilliam, E.A., and Li, L. (2014). Innate immune programing by endotoxin and its pathological consequences. Front. Immunol. *5*, 680. https://doi.org/10.3389/fimmu.2014.00680.
74. Yi, Z., Geng, S., and Li, L. (2023). Comparative analyses of monocyte memory dynamics from mice to humans. Inflamm. Res. *72*, 1539–1549. https://doi.org/10.1007/s00011-023-01762-8.
75. Yuan, R., Geng, S., and Li, L. (2016). Molecular Mechanisms That Underlie the Dynamic Adaptation of Innate Monocyte Memory to Varying Stimulant Strength of TLR Ligands. Front. Immunol. *7*, 497. https://doi.org/10.3389/fimmu.2016.00497.
76. Foster, S.L., Hargreaves, D.C., and Medzhitov, R. (2007). Gene-specific control of inflammation by TLR-induced chromatin modifications. Nature *447*, 972–978. https://doi.org/10.1038/nature05836.
77. Fitzgerald, K.A., Rowe, D.C., Barnes, B.J., Caffrey, D.R., Visintin, A., Latz, E., Monks, B., Pitha, P.M., and Golenbock, D.T. (2003). LPS-TLR4 signaling to IRF-3/7 and NF-kappaB involves the toll adapters TRAM and TRIF. J. Exp. Med. *198*, 1043–1055. https://doi.org/10.1084/jem.20031023.
78. Saeed, S., Quintin, J., Kerstens, H.H.D., Rao, N.A., Aghajanirefah, A., Matarese, F., Cheng, S.C., Ratter, J., Berentsen, K., van der Ent, M.A., et al. (2014). Epigenetic programming of monocyte-to-macrophage differentiation and trained innate immunity. Science *345*, 1251086. https://doi.org/10.1126/science.1251086.
79. Sun, S., Aguirre-Gamboa, R., and Barreiro, L.B. (2023). Transmission of stimulus-induced epigenetic changes through cell division is coupled to continuous transcription factor activity. Front. Immunol. *14*, 1129577. https://doi.org/10.3389/fimmu.2023.1129577.
80. Caldwell, B.A., Wu, Y., Wang, J., and Li, L. (2023). Altered DNA methylation underlies monocyte dysregulation and innate exhaustion memory in sepsis. Preprint at bioRxiv. https://doi.org/10.1101/2023.08.30.555580.
81. Maheshwari, D., Kumar, D., Jagdish, R.K., Nautiyal, N., Hidam, A., Kumari, R., Sehgal, R., Trehanpati, N., Baweja, S., Kumar, G., et al. (2022). Bioenergetic Failure Drives Functional Exhaustion of Monocytes in Acute-on-Chronic Liver Failure. Front. Immunol. *13*, 856587. https://doi.org/10.3389/fimmu.2022.856587.
82. Huber, A., Killy, B., Grummel, N., Bodendorfer, B., Paul, S., Wiesmann, V., Naschberger, E., Zimmer, J., Wirtz, S., Schleicher, U., et al. (2020). Mycobacterial Cord Factor Reprograms the Macrophage Response to IFN-γ towards Enhanced Inflammation yet Impaired Antigen Presentation and Expression of GBP1. J. Immunol. *205*, 1580–1592. https://doi.org/10.4049/jimmunol.2000337.
83. Patwardhan, P., and Resh, M.D. (2010). Myristoylation and membrane binding regulate c-Src stability and kinase activity. Mol. Cell Biol. *30*, 4094–4107. https://doi.org/10.1128/mcb.00246-10.
84. Dagenais, A., Villalba-Guerrero, C., and Olivier, M. (2023). Trained immunity: A "new" weapon in the fight against infectious diseases. Front. Immunol. *14*, 1147476. https://doi.org/10.3389/fimmu.2023.1147476.
85. Gill, P.S., Ozment, T.R., Lewis, N.H., Sherwood, E.R., and Williams, D.L. (2022). Trained Immunity Enhances Human Monocyte Function in Aging and Sepsis. Front. Immunol. *13*, 872652. https://doi.org/10.3389/fimmu.2022.872652.
86. Pradhan, K., Geng, S., Zhang, Y., Lin, R.C., and Li, L. (2021). TRAM-Related TLR4 Pathway Antagonized by IRAK-M Mediates the Expression of Adhesion/Coactivating Molecules on Low-Grade Inflammatory Monocytes. J. Immunol. *206*, 2980–2988. https://doi.org/10.4049/jimmunol.2000978.
87. Geng, S., Chen, K., Yuan, R., Peng, L., Maitra, U., Diao, N., Chen, C., Zhang, Y., Hu, Y., Qi, C.-F., et al. (2016). The persistence of low-grade inflammatory monocytes contributes to aggravated atherosclerosis. Nat. Commun. *7*, 13436. https://doi.org/10.1038/ncomms13436.
88. Bernstein, D.L., Kameswaran, V., Le Lay, J.E., Sheaffer, K.L., and Kaestner, K.H. (2015). The BisPCR2 method for targeted bisulfite sequencing. Epigenet. Chromatin *8*, 27. https://doi.org/10.1186/s13072-015-0020-x.
89. Zhou, W., Triche, T.J., Jr., Laird, P.W., and Shen, H. (2018). SeSAMe: reducing artifactual detection of DNA methylation by Infinium BeadChips in genomic deletions. Nucleic Acids Res. *46*, e123. https://doi.org/10.1093/nar/gky691.

STAR★METHODS

KEY RESOURCES TABLE

REAGENT or RESOURCE	SOURCE	IDENTIFIER
Antibodies		
anti-Src	Cell Signaling	RRID:AB_10691385
anti-phospho-Src	Cell Signaling	RRID:AB_331034
anti-Syk	Cell Signaling	RRID:AB_2197223
anti-STAT1	Cell Signaling	RRID:AB_2198300
anti-phospho-Stat1 (Ser727)	Cell Signaling	RRID:AB_2197983
anti-TAX1BP1	Proteintech	RRID:AB_2198921
anti-PLAC8	Proteintech	RRID:AB_11182285
anti-Akt	Cell Signaling	RRID:AB_329827
anti-phospho-Akt 473	Cell Signaling	RRID:AB_329825
anti-β-actin	Cell Signaling	RRID:AB_2223172
HRP-conjugated anti-rabbit IgG antibody	Cell Signaling	RRID:AB_2099233
HRP-conjugated anti-mouse IgG antibody	Cell Signaling	RRID:AB_330924
anti-mouse CD16/32 (Fc blocker)	BD Biosciences	RRID:AB_394657
Human TruStain FcX	Biolegend	RRID:AB_2818986
APC-Cy7 anti-mouse CD11b	Biolegend	RRID:AB_830642
PE-Cy7 anti-mouse Ly6C	Biolegend	RRID:AB_1732093
APC anti-mouse PD-L1	Biolegend	RRID:AB_10612741
PE anti-mouse CD38	Biolegend	RRID:AB_312929
FITC anti- mouse CD86	Biolegend	RRID:AB_313149
FITC anti- human CD66b	Biolegend	RRID:AB_314495
PE-Cy7 anti- human CD14	Biolegend	RRID:AB_389353
APC-Cy7 anti- human CD16	Biolegend	RRID:AB_2562952
APC anti- human CD86	Biolegend	RRID:AB_493231
PE anti- human PD-L1	Biolegend	RRID:AB_940368
APC anti- human CD38	Biolegend	RRID:AB_2561902
FITC anti- human CD4	Biolegend	RRID:AB_312690
APC anti- human CD8	Biolegend	RRID:AB_312751
APC-Cy7 anti-CD69	Biolegend	RRID:AB_10679041
Chemicals, peptides, and recombinant proteins		
M-CSF	PeproTech	Cat#315-02
Lipopolysaccharide (LPS)	Sigma-Aldrich	Cat#L2630
Propidium iodide	Invitrogen	Cat#00-6990-50
Trehalose-6,6-dimycolate (TDM)	invivoGen	Cat#tlrl-tdm-1
Fetal bovine serum (FBS)	Peak	Cat#PS-FB1
Penicilin / Streptomycin	Gibco	Cat#15140122
GlutaMAX	Gibco	Cat#35050061
α-mycolic acid	Avanti	Cat#791280P
Methoxy-mycolic acid	Avanti	Cat#791281P
carboxyfluorescein succinimidyl ester	Invitrogen	Cat#C34554
anti-CD3 antibody	Bio X Cell	Cat#BE0001-1

(*Continued on next page*)

Continued

REAGENT or RESOURCE	SOURCE	IDENTIFIER
anti-CD28	Bio X Cell	Cat#BE0015-1
protease inhibitor Cocktail	Sigma	Cat#P5726, P0044, and P8340
Critical commercial assays		
NAD/NADH Quantitation Kit	Sigma-Aldrich	Cat#MAK037
Lactate Assay Kit	Sigma-Aldrich	Cat#MAK064
Bio-Rad DC Protein Assay kit	Bio-Rad Laboratories	Cat#5000112
ECL detection kit	VWR	Cat#490005-020
Experimental models: Organisms/strains		
C57BL/6 mice	The Jackson Laboratory	Cat#000664
TRAM$^{-/-}$ mice	Eltzschig Laboratory	N/A
TREM2$^{-/-}$ mice	Colonna Laboratory	N/A
Software and algorithms		
ImageJ software	NIH	https://imagej.nih.gov/ij/
FlowJo (v10)	BD Life Sciences	https://www.flowjo.com
Prism (v9)	Graphpad	www.graphpad.com
BD FACSDiva (v8.0.2)	BD Life Biosciences	www.bdbiosciences.com/en-us/products/software/instrument-software/bd-facsdiva-software
R (v4.2.0)	R Core Team	cran.r-project.org/bin/windows/base/
sesame (R package; v1.14.2)	Zhou et al.[8]	www.bioconductor.org/packages/release/bioc/html/sesame.html
Other		
Multiplex PCR Kit	QIAGEN	Cat#206143
PyroMark PCR Kit	QIAGEN	Cat#978703
RNeasy Plus Mini Kit	QIAGEN	Cat#175028095
Reverse transcription kit	Applied Biosystems	Cat#74134
PowerSYBR Green PCR Master Mix	Applied Biosystems	Cat#4367659

RESOURCE AVAILABILITY

Lead contact

Further information and requests for resources and reagents should be directed to and will be fulfilled by the Lead Contact, Liwu Li (lwli@vt.edu).

Materials availability

This study did not generate any new reagents.

Data and code availability

- The underlying numerical data Figures 1A–1H, 2A–2C, 2E, 3C–3F, 4A–4F, 5A–5F, 6D–6K, and 7F, and western blot original figures were deposited on Mendeley Data, and are publicly available as of the date of publication. Mendeley Data: https://doi.org/10.17632/bdgy79rt48.1.
- Raw and processed DNA methylation array data produced during this study are available through the Gene Expression Omnibus under the accession number: GSE242825.
- This paper does not report original code.
- Any additional information required to reanalyze the data reported in this paper is available from the lead contact upon request.

EXPERIMENTAL MODEL AND STUDY PARTICIPANT DETAILS

Animals and ethics statement

This study does not involve any *in vivo* animal procedures or experiments, and is solely limited to *in vitro* culture of harvested murine bone marrow cells from sex and age comparable mice (male and female, 6-12 weeks were used in this study). Leg bones from previously euthanized Trem2$^{-/-}$ mice with C57BL/6 background were kindly provided by Dr. Marco Colonna's group at Washington University. C57BL/6 mice originally from the Jackson Laboratory, Tram$^{-/-}$ (Ticam2$^{-/-}$) mice with C57BL/6 background from Dr. Holger Eltzschig at University of Texas Houston were bred and housed in the Virginia Tech Life Science 1 facility. All mice were in a controlled temperature at 23°C and 12 h light-dark cycle with *ad libitum* access to food and water. All animal procedures were in accordance with the U.S. National Institutes of Health Guide for the Care and Use of Laboratory Animals and approved by Institutional Animal Care and Use Committee (IACUC) of Virginia Tech.

METHOD DETAILS

Murine primary monocyte isolation and culture

Bone marrow was harvested from tibias and femurs of 6- to 12- weeks old mice with matched genders, and maintained in the 1640-RPMI media supplemented with 10% fetal bovine serum (FBS), 1% penicillin-streptomycin, and 1% L-Glutamine and 10 ng/mL M-CSF (PeproTech).[86,87] Cells were stimulated with PBS (negative control), high-dose LPS (HLPS, 100 ng/mL) in the presence or absence of methoxy mycolic acid (M-MA, 10 μg/mL) (Avanti), α-mycolic acid (α -MA, 10 μg/mL) (Avanti), or Trehalose 6,6′-Dimycolate (TDM, 10 μg/mL) (Invivogen) for 5 days at 37°C in a humidified 5% CO2 atmosphere. Treatments were given repeatedly with the same concentrations in conjunction with a changing media on day 1 and day 4. Bone marrow-derived monocytes cultured under such conditions were still monocyte-like and no mature macrophage marker CD71 expression, as previously established.[31]

Human monocyte culture

Human whole blood was purchased from PBS Research Blood Components. PBMCs were isolated using Ficoll-Paque PLUS (GE Healthcare Bio Science) and subsequently cultured in complete 1640-RPMI media. The media was supplemented with human M-CSF (PeproTech). Human PBMCs were then treated with LPS in the presence of without methoxy-MA at 0-h and 5-h time points and cultured for 1 day.

T Cell Isolation and coculture

Murine CD3$^+$ T cells were isolated from the spleen of C57BL/6 mice using the MojoSort Mouse CD3 T Cell Isolation Kit (Biolegend), yielding a purity of >95%. Isolated CD3$^+$ T cells were labeled with 5 μM carboxyfluorescein succinimidyl ester (CFSE; Invitrogen) for 8 min at room temperature (RT) and neutralized by 3 mL FBS for 10min at 37°C. CFSE-labeled T cells with the density of 1 × 10^6 cells/mL were resuspended in RPMI 1640 media supplemented with 10% PBS, 1% penicillin-streptomycin, 1% L-Glutamine, 10 mM HEPES, and 0.055 mM 2-mercaptoethanol. For monocyte-T cell coculture, pre-treated monocytes were washed with PBS twice, and a total of 1 × 10^5 cells/well of CFSE-labeled T cells were co-cultured with monocytes at a ratio of 1:1 in the U-bottom 96-well plates. These monocytes were pre-treated with either PBS, LPS, or a combination of LPS and M-MA for 5 days. Cells were maintained in the T cell culture conditioned media and exposed to 2.5 μg/mL of coated anti-CD3 antibody (Bio X Cell) and 2.5 μg/mL of soluble anti-CD28 antibody (Bio X Cell) for 2 days.

NAD and lactate assay

The NAD assay and lactate assay were performed using the NAD/NADH Quantitation Kit (Sigma-Aldrich) and Lactate Assay Kit (Sigma-Aldrich) in accord with the manufacturer's instructions. Intracellular NAD and lactate concentrations were measured using the spectraMax M2 Microplate Reader (Molecular Devices).

Western blot

Cell culture samples were collected and lysed in 2% SDS cell lysis buffer containing phosphatase inhibitor 2, phosphatase inhibitor 3, and protease inhibitor Cocktail (Sigma). Cell lysates were denatured at 95°C for 5 min. Bradford assay was performed to determine protein concentrations using the Bio-Rad DC Protein Assay kit (Bio-Rad Laboratories). Proteins were separated by size using electrical current through 10% acrylamide Gel and wet-transferred onto a PVDF membrane. Membranes were then blocked with 5% milk for 1h at room temperature. Post block, membranes were incubated with anti-Src (Cell Signaling), anti-phospho-Src (Cell Signaling), anti-Syk (Cell Signaling), anti-STAT1 (Cell Signaling), anti-phospho-STAT1 (Cell Signaling), anti-TAX1BP1 (Proteintech), anti-PLAC8 (Proteintech), anti-Akt (Cell Signaling), anti-phospho-Akt 473 (Cell Signaling), and anti-β-actin (Cell Signaling) primary antibody at 4°C overnight and secondary HRP-conjugated anti-rabbit IgG antibody (Cell Signaling) or HRP-conjugated anti-mouse IgG antibody (Cell Signaling) at room temperature for 1 hour. Images were developed with ECL detection kit (VWR). Relative protein expressions were quantified with ImageJ software (NIH).

Flow cytometry

Murine monocytes and human monocytes were harvest at day 5 or day 1 and blocked FcBlock (anti-mouse CD16/32, BD Biosciences or Human TruStain FcX, Biolegend) followed by stanning with mouse anti-CD11b (APC-Cy7, Biolegend), anti-Ly6C (PE-Cy7, Biolegend), anti-PD-L1 (APC, Biolegend), anti-CD38 (PE, Biolegend), anti-CD86 (FITC, Biolegend) or human anti-CD66b (FITC, Biolegend), anti-CD14(PE-Cy7,

Biolegend), anti-CD16 (APC-Cy7, Biolegend), anti-CD86 (APC, Biolegend), anti-PD-L1 (PE, Biolegend), anti-CD38 (APC, Biolegend) for 30 minutes. For monocyte-T cell coculture, T cells were blocked and stained with mouse anti-CD4 (FITC, Biolegend), anti-CD8 (APC, Biolegend), and anti-CD69 (APC-Cy7, Biolegend). Stained cells were washed with FACS buffer and resuspended into the FACS buffer containing Propidium Iodide (Invitrogen). MitoTracker™ Deep Red FM kit (Invitrogen) was used to detect mitochondrial potential as described by the manufacturer's instructions. Antibodies labeled samples were analyzed with a FACSCanto II (BD Biosciences), and data were analyzed with FlowJo (BD Life Sciences).

Quantitative RT-PCR

RNA extraction was isolated using the RNeasy Plus Mini Kit (QIAGEN), followed by cDNA synthesis using the reverse transcription kit (Applied Biosystems). Real-time PCR was performed using PowerSYBR Green PCR Master Mix (Applied Biosystems) on a CFX96 real-time PCR instrument (Bio-Rad Laboratories). The determination of relative expression levels for transcripts utilized the double ΔCT method and normalization to the expression of the housekeeping gene Bactin. Graphs and statistical analyses were conducted using GraphPad Prism v9.0.

Infinium Mouse Methylation BeadChip array

Genomic DNA was prepared from cultured monocytes using a DNeasy Blood & Tissue Kit (QIAGEN) and bisulfite (BS)-treated using an EpiTect Bisulfite Kit (QIAGEN). For Infinium Mouse Methylation BeadChip (Illumina) arrays, 500 ng of BS-treated DNA was processed and hybridized to individual array wells according to the manufacturer's protocol. BeadChip array signal was measured using the iScan System (Illumina). All samples were processed and run at the Children's Hospital of Philadelphia Center for Applied Genomics.

Bisulfite next-generation sequencing

A modified BisPCR[2] workflow was used to validate differentially methylated regions of interest identified on the Infinium array, as previously described.[80,88] Briefly, genomic DNA was bisulfite converted as described above and then used as a template for *Plac8* promoter enrichment using a PyroMark PCR Kit (QIAGEN). Amplified regions were pooled for column purification, and the purified pools were barcoded with Illumina indexing primers using a Multiplex PCR Kit (QIAGEN). All indexed pools for each sample were then pooled during column purification, after which library quality was determined using Tapestation DNA ScreenTape analysis (Agilent) at the Fralin Life Sciences Institute at Virginia Tech Genomics Sequencing Center. Finally, all indexed libraries were pooled with 6% PhiX spike-in DNA and sequenced using a MiSeq Reagent Nano Kit v2 (500 cycles) (Illumina) at the Fralin Genomics Sequencing Center.

Infinium BeadChip array analysis

Raw Infinium IDAT files were processed into corrected beta values using the openSesame pipeline (1.14.2; default parameters), and differentially methylated regions (DMRs) were identified using the sesame DML function.[89] PBS- and LPS-treated cultured bone marrow monocyte array values were previously published, but were collected and sequenced at the same time as M-MA samples.[80] Infinium BeadChip probe annotations, including transcription factor motif enrichment and chromatin state discovery and characterization (ChromHMM), were obtained using the sesame KYCG function. For gene ontology (GO) enrichment analysis, differentially methylated probes were matched to their nearest gene using sesameData_getGenesByProbes, and ontology enrichment was performed using the g:Profiler2 package (0.2.1). Average DNA methylation signal and unsupervised clustering heatmaps were prepared using the Rpackage pheatmap (1.0.12; https://www.rdocumentation.org/packages/pheatmap; clustering_method = "average"), and average signal violin plots were prepared using the Rpackage vioplot (0.4.0; https://github.com/TomKellyGenetics/vioplot). Principal components analysis (PCA) and Moods nonparametric median tests were performed using the R stats package.

BisPCR2 sequencing analysis

Sequenced reads were trimmed using Trim Galore (0.6.7; http://www.bioinformatics.babraham.ac.uk/projects/trim_galore) and mapped with Bismark (0.22.3; https://www.bioinformatics.babraham.ac.uk/projects/bismark) in paired-end mode. Non-deaminated reads were filtered out based on the presence of ≥ 3 consecutive instances of non-CG methylation (function: filter_non_conversion ; parameters: –paired –consecutive). Bedgraph files were prepared using the Bismark Methylation Extractor to calculate percent methylation at each CpG with ≥ 100x coverage. Aligned reads were converted to Bigwig tracks for UCSC browser visualization (http://genome.ucsc.edu).

QUANTIFICATION AND STATISTICAL ANALYSIS

GraphPad Prism v9.0 was used for graph generation and statistical analysis. Significance was determined using either one-way ANOVA followed by Tukey's post hoc test for multi-group comparisons or two-way ANOVA for analyses involving multiple factors. Statistically significant findings (p-values) are denoted as follows: *$p < 0.05$; **$p < 0.01$; ***$p < 0.001$.